Journal of Volcanology and Geothermal Research 460 (2025) 108284

Contents lists available at ScienceDirect

Journal of Volcanology and Geothermal Research

journal homepage: www.journals.elsevier.com/journal-of-volcanology-and-geothermal-research

Multiple dikes make eruptions easy

Agust Gudmundsson *

Department of Earth Sciences, Queen's Building, Royal Holloway University of London, Egham TW20 0EX, UK

ARTICLE INFO

Keywords:
Dike paths
Dike arrest
Dike propagation
Stress homogenisation
Eruption mechanics
Forecasting eruptions
Volcanic hazards

ABSTRACT

Dikes supply magma to most volcanic eruptions. Understanding how propagating dikes may, or may not, reach the surface is thus one of the fundamental tasks for volcanology. Many, perhaps most, dike segments injected from magma sources do not reach the surface to feed volcanic eruptions. Instead, the dike segments become arrested (stop their propagation), commonly at or close to contacts between mechanically dissimilar layers/units, at various crustal depths. This means that many and perhaps most volcanic unrest periods with dike injections do not result in eruptions. There are several conditions that make dike arrest likely, but the main one is layering where the layers have contrasting mechanical properties. Such layering means that local stresses are heterogeneous and anisotropic and, therefore, in some layers unfavourable for dike propagation – hence the dike arrest. Here I show that once a dike has formed, however, its very existence tends to make the local stress field along the dike homogeneous (with invariable orientation of principal stresses) and favourable (with dike-parallel orientation of the maximum compressive principal stress) for later dike injections. This means that subsequence dikes may use an earlier dike as a path, either along the margin or the centre of the earlier dike, thereby generating a multiple dike. Because earlier feeder-dikes form potential paths for later-injected dikes to the surface, many volcanic eruptions are fed by multiple dikes. Examples include recent eruptions in the volcanoes Etna (Italy) and Kilauea (Hawaii), and the Icelandic volcanoes Krafla, Hekla, Fagradalsfjall, and the Sundhnukur crater row. Thus, multiple dikes favour dike propagation to the surface; thereby making dike-fed eruptions easier.

1. Introduction

One of the basic goals of volcanology is to be able to predict with reasonable reliability the time and location of volcanic eruptions. While some eruptions have been forecasted, they are few and occur primarily in polygenetic (central) volcanoes that can be assumed to behave in essentially the same way before each eruption (Gudmundsson et al., 2022). The assumption that the behaviour of a polygenetic volcano does not change between eruptions may be valid for some volcanoes, but only for very short periods. This is because volcanoes are evolving dynamic systems that normally change greatly over time and may do so between successive eruptions. Such changes include those of the shape and size of the source magma chamber, the mechanical properties of the layers that constitute the volcano, the local stresses inside the volcano and, consequently, the likely paths of dikes during future unrest periods with magma-chamber rupture and dike injection.

Dikes supply magma to most eruptions on Earth (e.g., Galindo and Gudmundsson, 2012; Browning et al., 2015; Rivalta et al., 2015; Tibaldi, 2015; Elshaafi and Gudmundsson, 2016; Townsend et al., 2017; Drymoni et al., 2020; Gudmundsson et al., 2022). In the past decades there has been very great progress in monitoring dike propagation during unrest periods in volcanoes. The monitoring has primarily been through dense seismic networks (Passarelli et al., 2015; Agustsdottir et al., 2016) and, to a lesser extent, geodetic measurements, mainly GPS and InSAR (Dzurisin, 2006; Segall, 2010). Despite these high-technology networks and monitoring efforts of propagating dikes, successful forecasting of dike-fed eruptions is, as yet, rare – primarily because it is so difficult to provide reliable predictions as to the likely dike paths.

One reason for this difficulty is that many, and probably most, injected dike-segments become arrested on their path to the surface. This means that many dike-segments never reach the surface to supply magma to an eruption. Arrested dike-segments are commonly observed in the field (Geshi et al., 2010, 2012; Drymoni et al., 2020; Gudmundsson, 2022). Also, many arrested dike-segments have been inferred in recent unrest periods, some with eventual eruptions, in Iceland and elsewhere (e.g. Moran et al., 2011; Roman, 2023). Recent examples of arrested dike-segment injections include the 2004 Teide (Canary Island) injection, many dike-segment injections in Eyjafjallajökull (South

* Corresponding author.
E-mail address: Agust.Gudmundsson@rhul.ac.uk.

https://doi.org/10.1016/j.jvolgeores.2025.108284
Received 28 November 2023; Received in revised form 26 January 2025; Accepted 29 January 2025
Available online 3 February 2025
0377-0273/© 2025 The Author. Published by Elsevier B.V. This is an open access article under the CC BY license (http://creativecommons.org/licenses/by/4.0/).

Iceland) prior to the 2010 eruptions, most of the segments of the dike that fed the 2014–15 Bardarbunga-Holuhraun (Central Iceland) eruption, and many dike-segment injections (some deflected into sills) during and prior to the recent eruptions on the Reykjanes Peninsula (Iceland) at Fagradalsfjall 2021–2023 and at the Sundhnukur crater row 2023–2024 (Gudmundsson, 2020; Hobe et al., 2025; Troll et al., 2024; Iceland Meteorological Office, 2025). Some of these eruptions show that the main part of the dike – that is, most of the dike-segments – became arrested at shallow crustal depths while a comparatively small 'dike finger' eventually reached the surface to feed an eruption. In such eruptions, the maximum inferred total length (strike-dimension) of the arrested (segmented) dike at shallow depths may be tens of times greater than the maximum length of the volcanic fissure, namely the surface expression of the tiny 'dike finger' that reached the surface and fed the eruption.

While dike-segment arrest is common, there is also evidence that in some volcanoes and volcanic systems/fields dikes find it easier to reach the surface than in others. I propose here that one main reason for an easy path to the surface is that the local stress field along the potential path of the dike-segment is everywhere essentially the same and favourable for dike propagation. Such stress fields are most likely to develop where all the layers hosting the potential path of the dike have similar or the same mechanical properties. The result is stress homogenisation, which is much more common in basaltic edifices/shield volcanoes than in stratovolcanoes/composite volcanoes (Gudmundsson and Brenner, 2004, 2005; Gudmundsson, 2006; Gudmundsson and Philipp, 2006)). An easy way to homogenise the stress field from the source to the surface is through existing dikes. Later-formed dike-segments then follow an earlier-formed dike-segment to generate a multiple dike (Fig. 1).

The main objective of this paper is to demonstrate through theory and field observations of dikes in active and fossil volcanoes/volcanic systems that dike-segments injected as a part of a multiple dike find it easier (less energy transformed) to reach the surface and erupt than single-injection segments. I first explain how dikes in general select their paths, using theories from analytical mechanics and fracture mechanics as a basis and, in particular, why so many dike-segments become arrested and never reach the surface (remain non-feeders). Then I discuss how earlier-formed dike-segments to a degree homogenise the associated stress field and thus provide potential paths for later-formed dike-segments. Many examples of multiple dikes are provided and analysed, from fossil volcanoes and volcanic systems as well as from active ones, with a focus on recent eruptions fed by multiple dikes. Both the theoretical and observational results support the proposal that during unrest periods the formation of a multiple dike increases the chances of dike-fed eruptions.

Fig. 1. View northeast, a multiple regional basaltic dike in Northwest Iceland. Dikes in this area have an average thickness of about 4 m, and a common range in thickness from 1 m to 10 m. The dike is composed of many columnar rows.

2. Dike arrest and mechanical layering

The reason that many, and probably most, injected dike-segments do not research the surface to erupt is that they become arrested (Fig. 2). Dike arrest, which means that a dike-segment stops its vertical propagation, is normally caused by one or all of three main mechanisms or processes. These are (1) Cook-Gordon delamination, (2) stress barrier, and (3) elastic mismatch. The details of these arrest mechanisms are provided by Gudmundsson (2011a, 2020), but may be briefly summarised as follows.

When a dike propagates vertically towards a horizontal or gently dipping contact, the tensile stresses ahead of the dike tip may open up the contact. This is because tensile stress ahead of the dike tip acts not only perpendicular but also parallel with the dip-dimension of the dike, which is the essence of the Cook-Gordon delamination mechanism. For the contact to open, the induced dike-parallel tensile stress must reach the tensile strength of the contact; the lower the tensile strength the more likely the contact is to open up (Gudmundsson, 2011a, 2011b). On reaching an open contact, the dike may partly deflect into it to form a sill or, alternatively, simply stop its vertical propagation. Because contacts between layers at shallow depths tend to have lower tensile strengths than contact between similar layers at great depths (where compaction and secondary mineralisation commonly increases the contact tensile strength), this mechanism of dike arrest is most likely to operate at shallow crustal depths. The other two mechanisms, however, operate equally well at any crustal depth.

For a vertically propagating dike a stress barrier is a horizontal or gently dipping rock layer/unit with an unfavourable local stress field, that is, a layer/unit where the maximum compressive principal stress σ_1 and the intermediate compressive principal stress σ_2 are horizontal and the minimum compressive (maximum tensile) principal stress σ_3 vertical. On meeting a stress barrier, the dike cannot continue its vertical propagation, resulting in the dike deflecting into a sill or stopping its propagation altogether. For deflection into a sill, the driving pressure/overpressure of the dike must be high enough for the magma to propagate along the lower contact of the barrier. If, however, the driving pressure is too low for such a deflection to occur, the dike simply stops its vertical propagating on meeting with the lower contact of the barrier. Stress tends to be transferred to (concentrate in) stiff layers. It follows that when a dike approaches a contact between a comparatively compliant layer below the contact (and hosting the dike) and a much stiffer layer above the contact the dike may occasionally stop its vertical propagation at some distance below the contact (Fig. 3; Inskip et al., 2020).

The elastic mismatch mechanism reflects the difference in stiffness or Young's modulus between the layers/units above and below the contact in relation to the mechanical properties of the contact itself. For a horizontal or gently dipping contact, the greater the stiffness of the layer above the contact in comparison with the stiffness of the layer or unit below the contact and hosting the dike, the stronger is the tendency for the dike to either stop its vertical propagation on meeting the contact or become deflected along the contact to form a sill (Gudmundsson, 2011a, 2011b, 2020).

All these three mechanisms depend on mechanical layering; in particular the difference in stiffness between the layers that constitute the volcanic system/field or (polygenetic) volcano. That mechanical layering to a large degree controls dike arrest is in agreement with field studies (Figs. 2–3; Gudmundsson, 2011a, 2011b, 2020, 2022; Inskip et al., 2020; Drymoni et al., 2020; Corti et al., 2023). Mechanical layering, particularly at shallow depths, also affects dike-induced surface stresses and deformation (Gudmundsson, 2003; Al Shehri and Gudmundsson, 2018; Bazargan and Gudmundsson, 2019, 2020) and

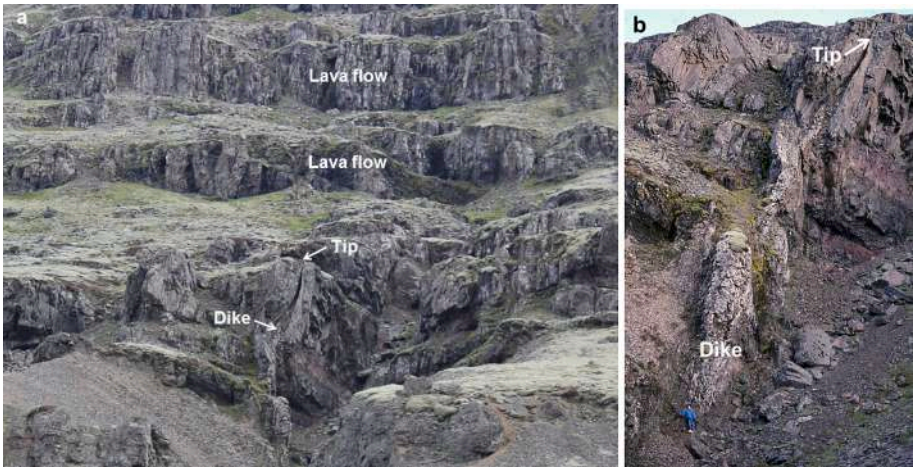

Fig. 2. Arrested basaltic dike in East Iceland. (a) View southwest, the exposed segment of the dike is arrested in a basaltic lava pile at a depth of about 1 km below the initial top of the pile. The tip is indicated. (b) Close-up of the arrested dike. At the base of the section seen here (where the person is standing) the dike is about 2 m thick, but thins upwards towards its tip where there was, during propagation, an empty cavity for a while (cf. Fig. 7).

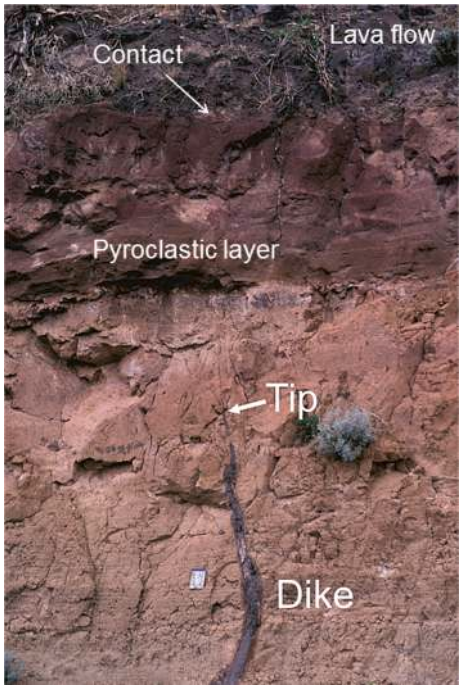

Fig. 3. Arrested basaltic dike in Tenerife (Canary Islands). View west, the dike thickness gradually decreases from 25 cm at the floor of the section to 2 cm at the vertical tip. The compliant (soft) pyroclastic host rock is thermally metamorphosed (baked) next to the dike. The tip of the dike became arrested within the compliant pyroclastic rock several metres below the contact with (the bottom of) much stiffer lava flow (cf. Inskip et al., 2020).

thus surface-deformation based calculations as to the depth to the tip (top) and thickness of arrested dikes. Mechanical properties of the layers/units that constitute a volcano/volcanic system thus largely control dike-propagation paths, dike arrest, dike-induced surface deformation and, therefore, associated volcanic hazards.

3. Dikes compared with human-made hydraulic fractures

Human-made hydraulic fractures, injected to increase the permeability of reservoirs, show great similarities with dikes as regards fracture paths, particularly deflection and arrest at contacts. In conventional hydraulic fracturing the hydraulic fracture is injected laterally into a target layer from a vertical well and supposed to stay within the target layer, that is, to become arrested (as regards its vertical propagation) at the top and bottom of that layer (Howard and Fast, 1970; Valko and Economides, 1995; Yew and Weng, 2014; Shapiro, 2018). Such hydraulic fractures reach strike-dimensions (horizontal lengths) of many hundred metres on either side of the well. Their mechanics of formation is analogous to those radial dikes that are injected partly or primarily laterally from shallow magma chambers (Fig. 4).

In unconventional hydraulic fracturing the fractures are injected

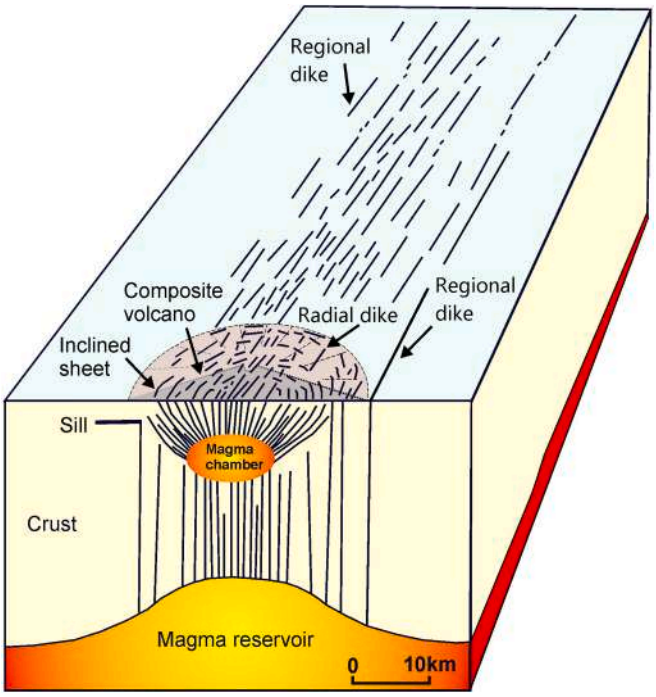

Fig. 4. Typical internal structure of a volcanic system supplied with magma through a double magma chamber, that is, a shallow crustal chamber whose source is a deeper and much larger magma reservoir. Thin radial dikes and inclined sheets are injected from the shallow chamber whereas the regional and thicker dikes (one of which here deflects into a sill) are mostly supplied with magma directly from the deep-seated reservoir. Dense sheet swarms develop close to shallow chambers, and their magmas, even if mostly basaltic, are more evolved than the basaltic magmas which erupt from the deep-seated reservoirs.

vertically into the rock layers from a horizontal well; this technique is primarily used for gas shales (Wu, 2017; Shapiro, 2018). The dip-dimension or height of some hydraulic fractures reaches a kilometre or more (Davis et al., 2012), but most are much shorter (Fisher and Warpinski, 2011; Fisher, 2014). The mechanics of formation of vertical hydraulic fractures is analogous to that of dikes formed in, partly or primarily, vertical propagation. The vertical and lateral dimensions of many radial dikes (Fig. 4) are similar to those of these hydraulic fractures.

During their propagation, dikes and hydraulic fractures generate earthquake swarms, mostly of microseismicity, making it possible to trace their propagation paths (Fisher and Warpinski, 2011; Davis et al., 2012; Flewelling et al., 2013; Fisher, 2014; Shapiro, 2018; Hobe et al., 2025). The microseismicity is largely attributable to fault slip in the walls of the fluid-driven fracture as well as to slip in the process zone ahead of the propagating fracture tip (Gudmundsson, 2011a, 2020; Geshi and Neri, 2014; Agustsdottir et al., 2016; Shapiro, 2018; Hobe et al., 2025). When the dike tip reaches close to the Earth's surface, the dike-induced stresses may reactivate or generate surface fractures and related deformation even if the dike itself, eventually, does not reach the surface (Al Shehri and Gudmundsson, 2018; Bazargan and Gudmundsson, 2019; Gudmundsson, 2020).

4. Dike-path selection

4.1. Hamilton's principle

I suggested earlier that dike-propagation paths are determined by the principle of minimum potential energy or least work (Gudmundsson, 1984, 1986). This principle is a reduced form of Hamilton's principle of least action, namely when the kinetic energy can be omitted. When applied to dike propagation, Hamilton's principle may be formulated so that of all the possible paths with the same initiation and termination points within the crust, the dike selects the path along which the time integral of the difference between the kinetic and potential energies is stationary (is an extremum) relative to all other potential paths. For most processes to which the Hamilton's principle applies the extremum turns out to be a minimum, which is what we assume here for dike and dike-segment paths.

The Hamilton's principle may be given as:

$$\delta S = \delta \int_{t_1}^{t_2} L dt = \delta \int_{t_1}^{t_2} (T - V) dt = 0 \quad (1)$$

Here, S is the action, L the Lagrangian, t_1 and t_2 two specified and arbitrary chosen times during the evolution of the system, and δ is the variational symbol, denoting a small change. Also, T denotes the kinetic energy and V the potential energy, so that the Lagrangian L is equal to the difference between the kinetic energy and the potential energy, namely:

$$L = T - V \quad (2)$$

Hamilton's principle (Eq. 1) states that when a system (here a discrete one) moves from time t_1 to time t_2 the actual path chosen is the one that makes the variation of the action δS zero. The actual path taken is thus the one for which the action integral (Eq. 1) is an extremum, here assumed a minimum, along the chosen path. The dimensions of action are energy × time (or linear momentum × distance), the unit being J s (joule-second). Hamilton's principle therefore implies that of the infinite number of possible dike paths (Fig. 5), the chosen path is characterised by the energy transformed multiplied by the time taken for the dike propagation being a minimum, that is, being least.

Eq. (1) applies to discrete and conservative systems. Discrete means that the system is composed of (normally numerous) particles. Conservative means that work done by a force is independent of path

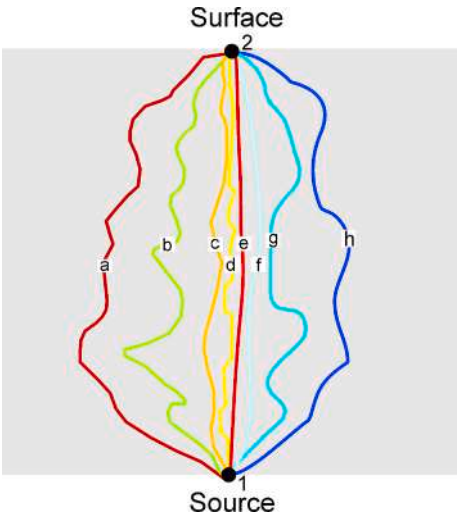

Fig. 5. Dikes (and inclined sheets) initiated at a source chamber/reservoir can, theoretically, select among an infinite number of paths to reach the surface (or the point or line of dike arrest within the crust). The point of source rupture and dike initiation is here denoted by 1 and the surface (for a feeder-dike; alternatively the point or line of arrest within the crust) by 2. Only 8 paths (denoted a-h) are shown here, however. From Hamilton's principle of least action it follows that a dike chooses the path along which the time integral of the difference between the kinetic and potential energies is stationary (is an extremum), and most commonly a minimum, relative to all other possible paths with the same points of initiation and eruption (or arrest; cf. Gudmundsson, 2020).

(reversible) within the system and is also equal to the difference between the final and initial values of the potential energy (potential energy function). In a conservative system the force field can then be expressed as a gradient of the potential energy (also named the potential). The system itself is conservative when all the forces acting on it are conservative. In many solid-mechanics models, including some for crustal segments, the external forces or loads are such that the body forces and the surface stresses are independent of the solid-body deformation (Fung and Tong, 2001). This implies that there is no friction in the system. Friction is very important in faulting (shear-fracture development). Most dikes are extension fractures (mode I cracks), however; they are thus generated by pure opening so that possible friction between the fracture walls is of less importance (Gudmundsson, 2020).

4.2. Hamilton's principle for a continuous system

A crustal segment hosting a propagating dike is composed of rock layers/units that constitute a continuous rather than discrete system. To a first approximation, the crustal segment is also an elastic system. Continuous and discrete systems in this context refers to their degrees of freedom, which indicate the minimum number of independent coordinates required to specify completely the configuration of a system that is also compatible with any imposed constraints. Configuration refers to the position, at a given moment, of all the particles of a discrete system or all the material points of a continuous system (Reddy, 2002). Here the degrees of freedom mean the number of independent parameters needed to define the configuration of the system. A discrete system of N particles without constraints has 3 N degrees of freedom. While N may be very large, it is always finite in a discrete system. In a continuous system, however, N is infinite, implying that the degrees of freedom of a continuous system are infinite.

In a discrete mechanical system, the potential energy V depends solely on the external forces (loading) or force field, such as gravity. In a continuous elastic system, here a crustal segment, there is, in addition to the potential energy of the external forces (loading), an internal strain

energy, attributable to internal forces stored in the elastic rock surrounding the source magma chamber before the chamber roof ruptures and a dike-segment is injected. When there is magma-chamber inflation, strain energy concentrates in the roof and the walls of the chamber, and also in the associated volcano itself, before a dike-segment is injected. When the generalised external forces Q_i are derivable from potential energy V (and thus conservative) then:

$$Q_i = -\frac{\partial V}{\partial q_i} \tag{3}$$

where q_i denotes generalised coordinates. The Hamilton's principle of least action for a crustal segment modelled as an elastic solid may be presented as follows (Tauchert, 1981; Bedford, 1985; Reddy, 2002):

$$\delta S = \delta \int_{t_1}^{t_2} (T - V - U)dt = 0 \tag{4}$$

Here δ is the variational symbol, S the action, T the kinetic energy, V the potential energy (due to the generalised external forces in Eq. 3 acting on the elastic rock body), and U the strain energy that has concentrated (accumulated) in the crustal segment which hosts the expanding (inflating) magma chamber. We assume that there are no constraints and that the external forces acting on the crustal segment hosting the chamber are independent of the elastic displacements that they generate, that is, are conservative (Eq. 3) – a common assumption for elastic deformation (Tauchert, 1981; Fung and Tong, 2001).

The strain energy stored in the crustal segment hosting the magma chamber and the potential energy attributable to the external generalised forces acting on the body are known together as the total potential energy Π, so that:

$$\Pi = V + U \tag{5}$$

The Lagrangian (Eq. 2) may then be written as:

$$L = T - \Pi \tag{6}$$

and Hamilton's principle (Eq. 4) becomes:

$$\delta S = \delta \int_{t_1}^{t_2} (T - \Pi)dt = 0 \tag{7}$$

4.3. Reduction of least action to the minimum potential energy principle

When a dike propagates there is normally an associated earthquake activity. The rate of dike propagation, however, is much lower than the rate of propagation of seismic ruptures. Seismic ruptures commonly propagate at rates similar to those of S-waves, that is, typically at between 2 km s^{-1} and 4 km s^{-1} in the solid upper crust. Thus while earthquake ruptures in the crust normally propagate at the rate of kilometres per second dikes commonly propagate (as magma-filled fractures) at rates from centimetres to, at most, metres per second. Here are some examples:

- During dike injections in the Krafla volcanic system, Iceland, from 1975 to 1984, the rate of dike-induced earthquake migration was mostly between 0.4 m s^{-1} and 1.2 m s^{-1} while the rate of lateral surface-fissure (feeder-dike segment) propagation was from 0.1 m s^{-1} to 0.4 m s^{-1} (Gudmundsson, 1995a).
- In the dike-emplacement episode in the Manda Hararo-Dabbahu spreading centre in Africa from 2005 to 2010, the inferred rate of dike-induced earthquake migration was from 0.14 m s^{-1} to 0.63 m s^{-1} (Grandin et al., 2011).
- Dike propagation rates in the volcano Etna (Italy) – not as inferred from earthquake migration but rather from the migration of surface fracturing – has been estimated at 0.02 m s^{-1} to 0.46 m s^{-1} (Falsaperla and Neri, 2015).
- Earthquakes migrated some 48 km in 13 days prior to the Bardabunga-Holuhraun eruption in 2014 at an average rate of 0.04 m s^{-1} (Gudmundsson et al., 2014).
- For the propagation of two injected dike segments that eventually reached the surface to supply magma to the 2021 Fagradalsfjall eruption in Iceland the rate of vertical propagation was about 0.02 m s^{-1} (Hobe et al., 2025).
- Some of the highest recorded rates of dike propagation, however, are those of primarily vertical dike propagation in Piton de la Fournaise in Reunion (France). There rates as high as 2 m s^{-1} have been reported whereas for lateral dike propagation in the same volcano the rates vary between 0.2 m s^{-1} and 0.8 m s^{-1} (Peltier et al., 2005).

The slow rate of propagation of typical dikes, as magma-filled fractures, means that when analytical and numerical models of dikes are made static rather than dynamic elastic moduli (such as Young's modulus) are normally used (Gudmundsson, 2011a). The slow propagation also implies that the kinetic energy transformed during typical dike propagation is comparatively small. If the transformed kinetic energy can be regarded as effectively zero then $T = 0$. If, additionally, the hosting crustal segment is behaving as a conservative, elastic system, then it can be shown (Richards, 1977; Tauchert, 1981; Reddy, 2002) that when in equilibrium, the total potential energy of the system is a minimum, thus:

$$\delta(V + U) = \delta\Pi = 0 \tag{8}$$

where V is the potential energy due to the generalised external forces, U the strain energy due to the internal forces, and Π the total potential energy. Eq. (8) represents the principle of minimum potential energy, stated as follows: Of all the possible configurations or displacement fields of an elastic body that satisfy both the external and internal loads as well as the constraints, the actual displacements are those that make the body's total potential energy a minimum. This means that for an elastic body to be in stable equilibrium, it is necessary and sufficient that the total potential energy of the body be a minimum.

The principle of minimum potential energy (least work) was proposed as a basic idea for understanding dike paths by Gudmundsson (1984, 1986). Here that idea is extended and developed into a general theoretical framework for understanding and forecasting likely dike paths. Further details on the theory of modelling dike paths are provided by Gudmundsson (2020, 2022). The main point here is to show how formation of multiple dikes, that is, dikes resulting from several magma injections along partly or completely the same path, encourages dike-fed eruptions. Before we discuss the paths, a brief summary of the energy aspects of dike-fracture formation is warranted.

4.4. The selected path

The selected 'path' suggested by Hamilton's principle of least action normally refers to the one along which a system 'moves'. This implies that the 'path' reflects changes in its configuration rather than an actual movement of the entire system. Each location or point on the path along which the system moves through time then corresponds to one particular configuration of the system. Configuration here denotes the arrangement of the material points (for a continuous system) or the particles (for a concrete system). In the present paper, the use of Hamilton's principle (and its reduced version, the principle of minimum potential energy) is extended so that the discussed 'paths' refer to the actual dike-propagation paths. Similar assumptions are made when using phase-field models of fracture propagation (Bourdin and Francfort, 2008; Del Piero, 2013). As discussed later, however, the modelling of fractures using phase-field approach is very different from the approach used in the present paper. The phase-field approach is, at this

stage of development, not very suitable for modelling dike propagation.

The present extension of the earlier ideas as to the use of minimum-energy principles to model dike propagation improves our understanding of how dikes actually propagate. This improved understanding applies not only to the eventual paths that the dikes select, but also their propagation steps (Fig. 6). When the overpressure at the tip of a propagating dike reaches the condition for propagation (Gudmundsson, 2011a, 2020), the rock ahead of the dike tip ruptures and the fracture tip (Figs. 2, 3, 7) advances at the velocity of kilometres per second (similar to the S-wave velocity). The fracture tip, however, advances only for a short distance (commonly metres) and then stops and becomes temporarily or, if further propagation does not happen, permanently arrested (Figs. 2, 3).

The viscous magma moves (flows) much more slowly than the dike-fracture tip advances during each of its propagation steps. The dike-fracture front will be essentially empty for a period of time following each propagation step (Fig. 7) because the magma front needs some time to flow towards the fracture tip. As the magma flows into the empty (open) tip part of the dike-fracture and fills it, magmatic overpressure builds up until the dike-fracture tip can advance again, resulting in a new propagation step which is also regarded as developing in accordance with Hamilton's principle of least action (Eq. 7) or, alternatively, the principle of minimum potential energy (Eq. 8). For a crustal segment composed of layers/units the vertical dimension (height) of each step may be equal to the thicknesses of the layers/units ahead of the dike-fracture front (Figs. 2, 6). Each propagation step is then either confined to a single layer/unit, particularly if the layers/units are young and their contacts are of low tensile strength. As the pile of layers/units becomes older secondary mineralisation and compaction increases the tensile strength of the contacts between the layers/units, and at the same time the mechanical contrast between layers (primarily the difference in Young's modulus) decreases. Piles of older layers may thus sometimes function as single mechanical layers/units during dike propagation (Gudmundsson, 2020, 2022). But while the dike path through such thick layers/units may be comparatively straight (Figs. 6, 8) the dike-fracture front or tip cannot normally advance through very thick layers/units in a single step and would need several propagation steps to cut through.

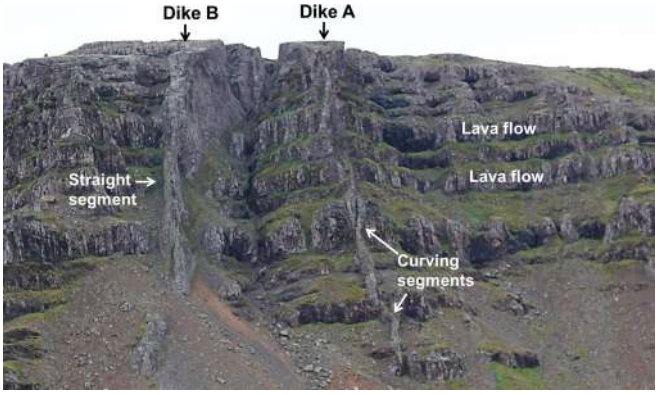

Fig. 6. Dikes propagate in steps, each step generating a segment. In many dikes the segments merge into large ones as the dike propagates and becomes thicker. Yet, the segments are clearly visible in some dikes, particularly those where the mechanical units (single layers or groups of layers) had somewhat different local stresses and/or tensile strengths at the time of dike emplacement (cf. Gudmundsson, 2022). Here dike A shows clear segments, some of which have different attitudes (are curving) from the overall attitude of the dike – indicating variation in the local stress fields/tensile strengths of the mechanical units cut by the dike. Dike B, while segmented, is comparatively straight, suggesting less variation (than for dike A) in local stresses/tensile strengths when it formed. Since layered crustal segments tend to become more homogenised in mechanical properties with time (partly through secondary mineralisation and compaction), dike B is presumably the younger one. View north, these basaltic dikes belong to a swarm in East Iceland (part of the swarm is seen in Fig. 8) with an average dike thickness of 5.5 m, but dike A is somewhat thinner than the average.

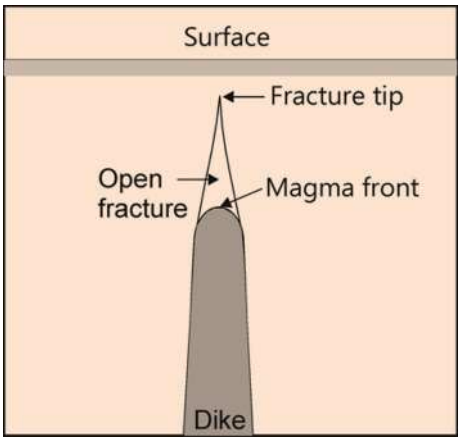

Fig. 7. During dike (magma-driven fracture) propagation the fluid front normally lags behind the fracture front or tip. At intervals during the propagation there will be an open unfilled fracture ahead of the fluid front. This conclusion is supported by field observations of dikes (Fig. 2) as well as field experiments and theories on human-made hydraulic fractures (Davis et al., 2012; Flewelling et al., 2013; Yew and Weng, 2014). Later on the fracture-driving fluid front 'catches up' with the fracture front.

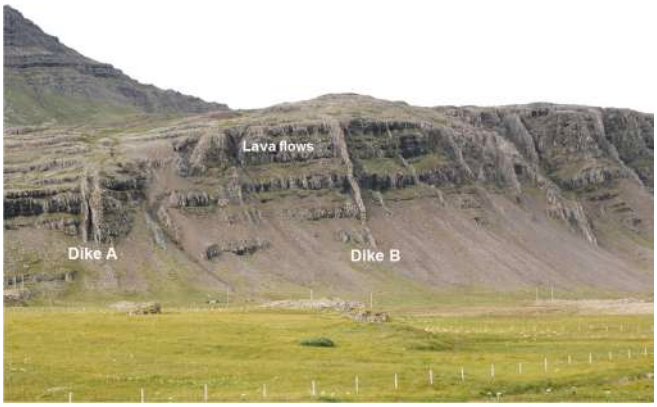

Fig. 8. Multiple dike (A) and apparently a single-injection dike (B) in the same swarm (in East Iceland) as seen in Fig. 6 (here many dikes are seen in addition to those indicated). View north, the swarm is composed of basaltic dikes that are here exposed at a depth of about 1.2 km below the initial top of the basaltic lava pile. The average thickness of dikes in the swarm is 5.5 m, and dike B is similar in thickness to the average but dike A is thicker. Many of the dikes, particularly dike B, follow comparatively straight paths through this section of the basaltic lava pile, indicating that this section functioned as a single mechanical unit when many of these dikes (but not the earlier dike seen in Fig. 6) were injected.

As a dike-fracture advances in steps (Figs. 2, 6), there are, theoretically, an infinite number of possible paths to select among – which also applies to the overall path of the dike (Fig. 5). The selected dike-propagation path from a location or point at time t_1 to the location or point at time t_2 is the one along which the action S or (when the kinetic energy is omitted) the potential energy Π is minimised.

5. Energy of dike propagation

For a dike to initiate and propagate, the host rock must receive surface energy to rupture the rock and create new fracture (walls or) surfaces (Anderson, 2005; Gudmundsson, 2011a). At an atomic level the surface energy is needed for two atomic planes to become separated to a

distance where there are no longer any interacting forces between the planes. For dike propagation the rupture is normally at the level of existing (often cooling/columnar) joints, pores, contacts, and other flaws in the host rock. Thus, the surface energy W_s is the energy that must be added to the hosting crustal segment so that a dike is can initiate and propagate. Because the energy is added to the rock (the thermodynamic system) it is regarded as positive.

For dike initiation and propagation the total energy U_t of the part of the crust hosting the dike must be large enough to overcome or balance the needed surface energy W_s. The total energy is composed of two parts (Sanford, 2003; Anderson, 2005): the surface energy and the total potential energy Π of the crustal segment. Therefore:

$$U_t = \Pi + W_s \tag{9}$$

As defined in Eq. (5) Π is the strain energy U plus the potential energy V. The potential energy V, in turn, is the derivative of the generalised forces Q_i (Eq. 3) which include body forces such as gravity and surface forces/stresses. The strain energy U is attributable to the internal forces between the material points in the deformed crustal segment. U becomes stored in part of the crust because of changes in the relative location of its material points (changes in the internal configuration) as that crustal part deforms and the material points become displaced. U is stored before the dike initiates and is thus available to drive the dike propagation, provided certain conditions are satisfied. The total strain energy U_t in a crustal part subject to deformation, such as inflation of a magma chamber, is stress × strain × volume and has the standard energy unit of joule. Dividing by volume, the strain energy per unit volume U_0 becomes:

$$U_0 = \int_V \frac{\sigma_{ij}\varepsilon_{ij}}{2} dV_v \tag{10}$$

Here, σ denotes stress and ε denotes strain, and the subscripts ij indicate the 9 components of the stress tensor and the strain tensor. The unit volume of the strained crustal segment is denoted by dV_v, with the subscript v standing for volume (V_v) so as to distinguish it from potential energy (V). If we drop the subscripts ij to simplify the notation and use Hooke's law (Gudmundsson, 2011a), from Eq. (10) the total strain energy U_t then becomes:

$$U_t = \frac{\sigma\varepsilon V_v}{2} = \frac{E\varepsilon^2 V_v}{2} = \frac{\sigma^2}{2E} V_v \tag{11}$$

where E is Young's modulus. Using Eq. (11) we can calculate the total strain energy stored in that volume V_v of the crust which is subject to deformation, such as during inflation of a magma chamber or a reservoir, prior to dike initiation and propagation. Once a dike is initiated and begins its propagation into the roof of the source chamber/reservoir, the strain energy (Eqs. 9 and 11) is partly transformed into the surface energy needed to form the two new dike-fracture surfaces, and partly into the energy driving microcracking and plastic deformation in the process zone at the tip of the propagating dike, as well as used for driving fracture (mainly joint) reactivation through fault slip in the dike walls.

A dike can propagate to a significant distance from its source, generating new surface area dA (of the dike-fracture walls), only if the total energy U_t (Eqs. 9 and 11) remains constant or decreases during the propagation. For equilibrium conditions, the dike can propagate if $U_t = k$, where k is a constant. From Eq. (9) and the condition $U_t = k$, we have:

$$\frac{dU_t}{dA} = \frac{d\Pi}{dA} + \frac{dW_s}{dA} = 0 \tag{12}$$

and therefore:

$$-\frac{d\Pi}{dA} = \frac{dW_s}{dA} \tag{13}$$

Eq. (13) shows that the decrease in total potential energy Π during dike propagation is equal in magnitude to the increase in surface energy W_s. The stored potential energy in a crustal segment transformed into surface energy during dike (or, in general, mode I crack) propagation is known as energy release rate, denoted by G and given by:

$$G = -\frac{d\Pi}{dA} \tag{14}$$

where G may be viewed as the energy available to drive dike propagation. A dike propagates only if the energy release rate G reaches the critical value on the right-hand side of Eq. (13), that is:

$$G_c = \frac{dW_s}{dA} \tag{15}$$

where the critical value G_c is the material toughness of the host rock of the dike (Anderson, 2005; Gudmundsson, 2011a, 2020).

6. Stress-field homogenisation and multiple dikes

6.1. Stress-field homogenisation

An existing dike essentially homogenises temporarily the stress field from the source to the tip of the dike. I proposed earlier that stress homogenisation is a major reason for fractures reaching great lengths; the proposal applies both to faults as well as dikes (Gudmundsson and Homberg, 1999; Gudmundsson and Brenner, 2004, 2005; Gudmundsson, 2006; Gudmundsson et al., 2010). In this section, I first discuss how this homogenisation takes place, and then present some examples of multiple dikes as seen in the field and discuss how and under what conditions they form.

A stress field is defined as homogenised if the orientations (but not the magnitudes) of the principal stresses are everywhere the same. A perfect homogenisation is rarely achieved in heterogeneous and anisotropic rocks, but the stress field may be similar enough to favour the propagation of a dike. To encourage dike propagation, the orientation of the principal stresses must not only be the same along the potential dike path but, in addition, the maximum principal compressive stress, σ_1, must be parallel with the dip-dimension of the dike (essentially vertical).

When an earlier dike path is already established, it affects, and normally encourages, subsequent dike-segment injections in several ways. First, the path from t_1 to t_2 is already following the principle of least action (Eqs. 4 and 5) so that further dike-segment injections tend to use the path so as to minimise the action or, when the kinetic energy is omitted, the total potential energy (Eq. 8). Second, the injected earlier dike tends to homogenise the stress field along its path. This is because the dike rock is everywhere the same along the path. Thus orientation of the principal stresses inside and along the dike tends to be similar from the dike source to its tips. While the homogenisation is hardly ever perfect, particularly not in a layered crustal segment where the layers have widely different mechanical properties, yet the dike rock itself, being of essentially the same mechanical properties along its entire path, tends to smooth out the mechanical, hence the stress-orientation, variations. Third, the injected earlier dike provides a constraint on the potential paths of later dike-segment injections. Both the margins (the contacts between the dike and the host rock) and the centre of the earlier dike offer weaknesses that may function as paths for later dike injections. These primarily follow the centre (the last part of the dike to solidify) and the margins of the earlier dike and, thereby, offer constraints on the path of the subsequently injected dike-segments that follow the earlier dike. Fourth (which is related to the third point) the rock tensile strength along the margins and the centre of the earlier formed dike tends to be low along the entire dike, thereby further encouraging later dike injections to use these as paths. It is important that the low tensile strength is continuously so along the dike. There is low tensile strength in the layers of the host rock, particularly cooling/columnar joints in lava flows (Figs. 1, 2, 6, 8). But the low strength in such a pile is not continuous in a vertical section; contacts and layers of scoria, tuff, and soil disrupt the continuity of the potential paths of low

tensile strength, at which dike-segments commonly become either offset or permanently arrested (Figs. 2, 3, 6; Gudmundsson, 1986, 2022). In contrast, the low tensile strength is continuous along the margins or centre of the earlier dike.

A dike that is not a part of a multiple dike has normally to propagate through many rock layers. Such layers have commonly widely different mechanical properties and local stresses that are unfavourable to dike propagation. Thus, dike arrest (Figs. 2, 3), or dike deflection into a sill, is very common. By contrast, once a dike-path has formed as a result of an earlier dike propagating through numerous mechanical layers, it is commonly easier for subsequent dike-segments to propagate along the same path than to form a new path. Based on the above considerations, some of the main reasons why dike injections along existing dikes, namely the development of multiple dikes, are favoured may be summarised as follows.

- An earlier dike injection normally follows a path along which the action, or the potential energy, is minimised. There is thus a general tendency for later-injected dike-segments to follow that path, provided the later segments are initiated anywhere comparatively close to, or at the location of, the earlier injection so as to be able to join the earlier injection.
- The dike rock has everywhere essentially the same mechanical properties, resulting in the dike rock encouraging stress homogenisation.
- Stress concentration at the margin of the dike, that is, at its contact with the host rock, often resulting in fractures and low tensile strength along the margin, providing a potential path for a new dike-segment injection.
- The mechanically weak (low tensile strength) central part of the dike, namely the part that is the last one to solidify and cool down to the temperature of the host rock, also provides a potential path for a new dike-segment injection.
- If the new dike injection occurs inside the previous one, particularly along its centre, then the previous injection, if still hot, may thermally insulate the new dike injection from the host rock and, thereby, help its magma to maintain a relatively low viscosity.

6.2. Field observations of multiple dikes

Multiple dikes are very commonly observed in the field. Some typical ones are described below. In most cases it is not known if they were feeder-dikes, but the excellent exposures of many of them indicate the general structure of multiple dikes. Multiple dikes that acted as feeders are described in Section 7.

The best-known examples of dikes formed in many injections into the same fracture, and the ones easiest to recognise in the field, are composite dikes. The classic example of a composite dike is where the central part is acid and the marginal parts basaltic (Fig. 9). In composite dikes there is strong contrast in the composition/lithology of the magma injections (Fig. 10). The acid part does not have to be in the centre – it can be at the margin of a basaltic part – but commonly it is in the centre (Fig. 9). This is in agreement with the theory of the formation of multiple dikes, namely that the later dike-segments may be injected either along the margin of the earlier dike or along its centre. In rare cases can it be demonstrated that the composite dike was a feeder to composite lava flow (Fig. 10; Gibson and Walker, 1963).

Multiple dikes, where all the parts have similar composition/lithology, are much more common than composite dikes. For example, it is estimated that in parts of the Palaeogene Skye Central Complex (a fossil volcanic system in West Scotland), some 60 % of the basaltic dikes are multiple; and multiple dikes are also very common in other fossil volcanic systems in West Scotland such as on Mull and Arran (Emeleus and Bell, 2005). In many dike swarms in Iceland most of the thicker dikes are multiple, that is, composed of many parallel rows of columns. This applies particularly to basaltic dikes, who are commonly composed of 3–9 (or more) columnar rows (Figs. 1, 8, 11–14). While some multiple dikes are very thin (Fig. 13), many are thick (Figs. 1, 11, 12), and some very thick. For example, one of the thickest measured dikes in Iceland is multiple (Fig. 14), and the same applies to the dikes in Tenerife, Canary Islands (Fig. 15).

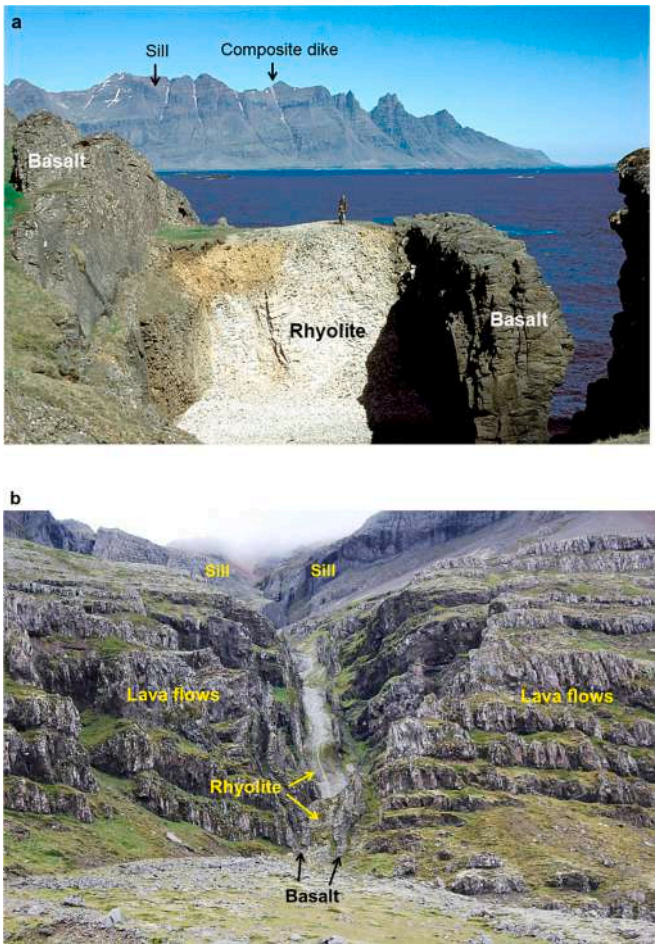

Fig. 9. Composite dikes, as seen here in East Iceland, are generated through the propagation of magmas of contrasting composition (here mafic and felsic) along the same path. (a) View north, the thickness of the rhyolite part is 13 m, that of the western basalt part 7.5 m, and that of the eastern basalt part 5 m; the total thickness to thus 25.5 m. The dyke (which is partly under the sea) can be traced along strike for about 14 km, its strike changing from N20°E here to N14°E towards its northern end. The dike extends to the top of the 700 m high mountain on the other side of the cove Breiddalsvik (seen here), but the basaltic parts drop out in the middle part of the mountain so that at the top the dike is purely acid and 35 m thick. A 120-m-thick multiple sill dissects the dike (also seen in b and in Fig. 17), and is thus younger than the dike. (b) At the entrance (bottom) to the gully (marked as 'composite dike' in a) the total thickness of the dike is 11 m. Here the dike is divided into four parts or columnar rows, two felsic (6 m and 1.5 m thick) and two mafic (1.5 m and 2 m thick). A short distance (to the north) into the gully, the dike reaches 13 m in total thickness, but is there composed of seven parts, four mafic and three felsic. These results, and others on multiple mafic dikes, show that multiple/composite dikes may vary in thickness and number of parts or columnar rows along their dip and strike dimensions.

Dikes are not the only sheet-like intrusions that are formed by many magma injections. Many inclined sheets (Fig. 16) and sills show clear evidence of being multiple (Browning and Gudmundsson, 2015; Thiele et al., 2021). This applies both to basic/mafic inclined sheets and sills (Fig. 17) and intermediate and felsic sheets and sills (Figs. 16, 18). When the columnar rows are very clear (Figs. 16, 17) it means that the earlier magma injection solidified before the next one was injected. Since the

Fig. 10. Composite feeder-dike (indicated) to the composite lava flow (indicated) of Raudafell in Berufjördur in East Iceland. View northeast, the composite dike is about 7 m thick. The composite lava flow is described by Gibson and Walker (1963).

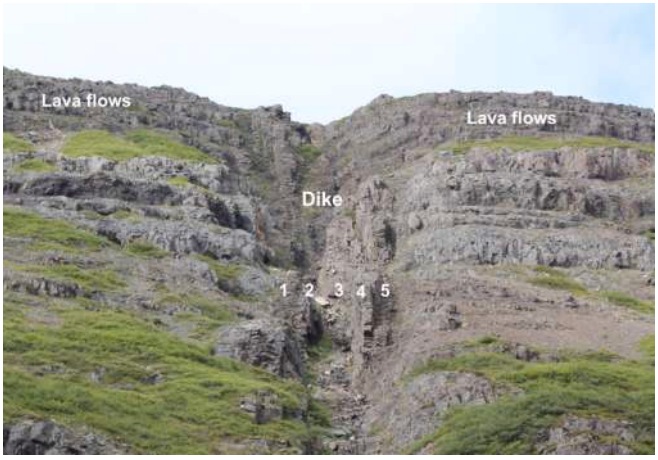

Fig. 11. View west, a multiple basaltic dike in Northwest Iceland. The dike is composed of many columnar rows (5 are indicated), is close to vertical, and with a total thickness of many metres. For comparison, the average thickness of dikes in Northwest Iceland is about 4.3 m and the common range in thickness is from less than 1 m to about 13 m (Gudmundsson, 1995b).

Fig. 12. Multiple basaltic dike in North Iceland. View northeast, the dike is composed of many columnar rows (seven are indicated) and reaches a total visible thickness of 20 m. The person provides a scale.

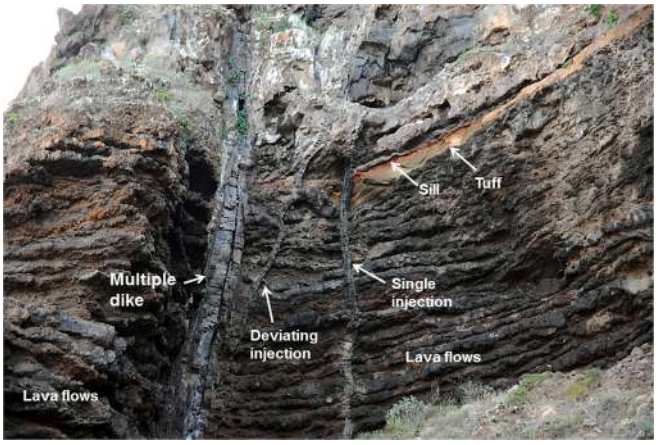

Fig. 13. Multiple basaltic dike in Tenerife (Canary Islalands). Part of the dike seen here is composed of three columnar rows or sheets, but the lower part of four to five rows. It is commonly seen when multiple dikes are followed along dip-dimension (like here) or strike-dimension (like the dikes in Figs. 9 and 14) that some of the columnar rows may deviate (indicated) from the main part for part of the path (and thus with host rock inbetween the rows), and then joint the other rows again (as seen here). The singje injection dike deflects partly into a sill (indicated) at the contact between the compliant tuff and a stiff lava flow. View south, the maximum thickness of the main dike is a few metres (photo: Kevin D'Souza).

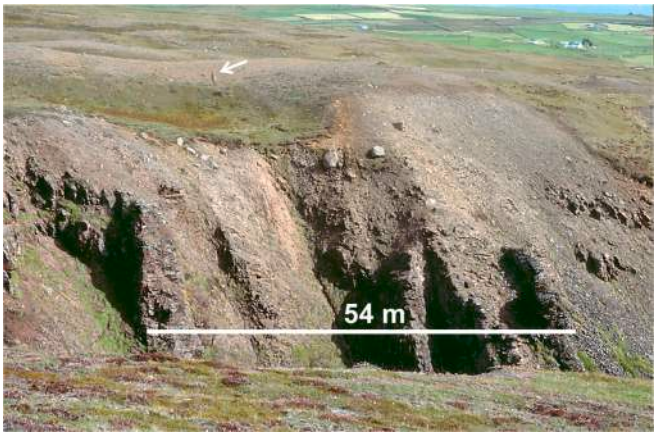

Fig. 14. Multiple basaltic dike in North Iceland. The dike is composed of at least three thick parts (presumably each merged from several rapidly injected thinner injections) or columnar rows and reaches a total thickness of 54 m. In this outcrop, the dike is seen as a single multiple dike, with no host rock in-between the parts. When the dike is followed along its strike, however, the three parts deviate (separate), meaning that there is host rock in-between the parts. In outcrops where there is host rock in-between the parts (the columnar rows), the dike would be considered three separate dikes. As discussed above (Figs. 9 and 13), commonly some later-formed dike injections (seen today as columnar rows) deviate somewhat from the path established by the earlier injections along part of the path of the multiple dike, often because of small variations in the local stress field, even if that field is close to homogenised by the first dike injection. View north, the white arrow points to a person for scale.

rate of cooling, hence of solidification, of a sheet depends on its thickness in the 2nd power, it follows that thin magma injections solidify quickly. For example, for a basaltic sill (or a dike) whose range of solidification is 1200–1000 °C, as is common, then a magma injection of thickness 1 m would solidify in less than 7 days and an injection of thickness 2 m would solidify in about 27 days (Gudmundsson, 2020). The cooling (columnar) joints form much later. For a 2 m thick basaltic magma injection, the joints would begin to form only after some 280 days.

Fig. 15. Multiple phonolitic dike in the Las Canadas caldera of Tenerife (Canary Islands). View north, the dike is composed of many columnar rows (some indicated) and has a thickness of many tens of metres.

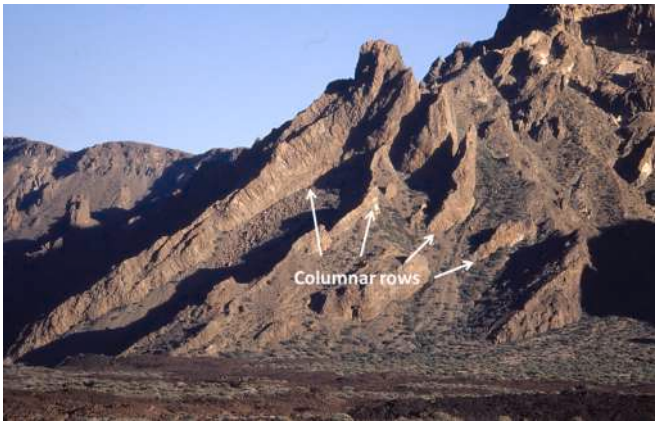

Fig. 16. Multiple phonolitic inclined sheet in the Las Canadas caldera of Tenerife (Canary Islands). View east, the total thickness of the multiple sheet is tens of metres.

Fig. 17. Multiple basaltic sill, 120 thick (only a part is seen here) in East Iceland. This part of the sill is composed of at least 16 columnar rows or sheets (three are indicated), some of which are also seen in Fig. 9b. The overall shape of the sill is concave upwards (Fig. 9a). At the time of its emplacement the sill was about 800 m below the surface of the active volcanic system. The exposed lateral dimension of the sill is about 3 km, but its initial lateral dimension is unknown. The 35-m-thick entirely felsic top of the composite dike in Fig. 9 is indicated.

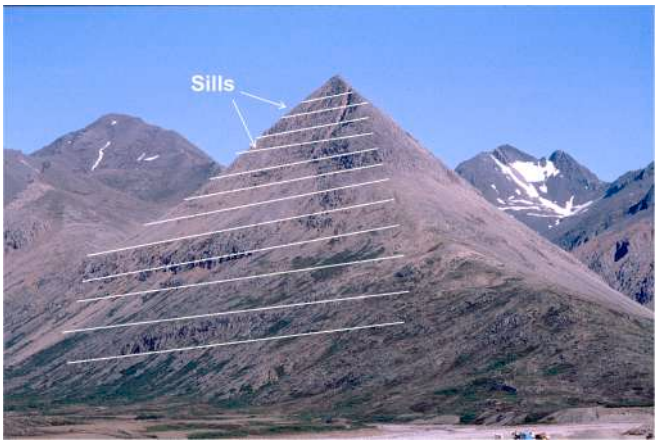

Fig. 18. Felsic (granophyre) sills constituting the fossil shallow magma chamber of Slaufrudalur in Southeast Iceland. Most of the sills are 15–50 m thick. The deepest exposed part of the magma chamber is about 2 km below the original top of the polygenetic (central) volcano to which it acted as a magma source (cf. Gudmundsson, 2020).

With reference to these field observations, the general way that multiple dikes form may be illustrated as follows (Fig. 19). Thin dikes composed of one columnar row (Fig. 20) are normally formed in a single magma injection. Thicker dikes, even if apparently composed of only one columnar row (Fig. 8), do not necessarily form in only one magma injection. This is because the columnar joints (and rows) for basaltic dikes begin to form only when the dike has cooled down from about 1200–1300 °C to about 700–800 °C. As indicated above, for a 2 m thick dike injection the cooling joints do not begin to form until after some 280 days.

In some dikes the central row has curved or upward-bent columns (Fig. 21). This curvature may indicate a later magma injection along the central part of an earlier dike. The curved columns suggest later

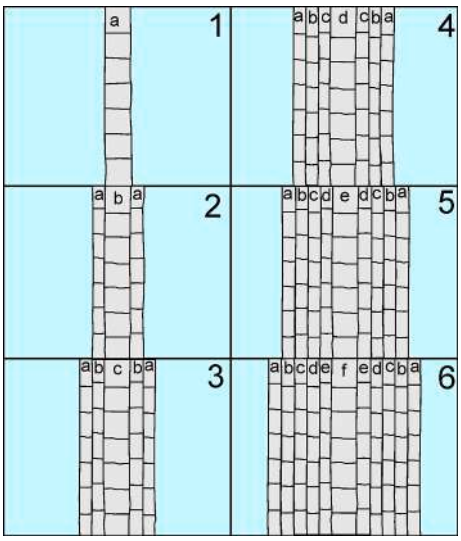

Fig. 19. Schematic illustration showing the formation of a multiple dike eventually composed of 11 columnar rows. (1) The first magma injection, resulting in the formation of columnar row a. (2–6) The subsequent magma injections (a-f) are here shown as using the mechanically weak central part of previous injections as paths. However, some or all the subsequent magma injections may occur at the margins of the previous ones, that is, at the contact between the dike and the host rock. If the time between successive magma injections is very short in relation with the thicknesses of the injections, the injections may merge into a single, thicker columnar rows or sheets, such as seen in Fig. 14.

Fig. 20. Single magma injection forming a dike composed of a single columnar row. View northeast, this mafic dike in West Norway is 0.7 m thick.

Fig. 21. Regional basaltic dike in Northwest Iceland with three columnar rows, suggesting a maximum of two main magma injections. The upward bending of the central columns in this segment may indicate late-stage movement of the (by then partly solidified and thus 'plastic') magma (Gudmundsson, 1986).

movement and/or the effects of water circulation in the central part of the dike after the outer parts had already cooled down to form columnar rows. There is, additionally, plenty of evidence that many dikes with only two to four columnar rows are formed in two or more separate magma injections (Figs. 1, 8, 13, 14). Then the columnar rows may be different in appearance (texture) and with somewhat different lithology (even if all are basaltic), such as in Figs. 1, 8, 13, and 14, or, alternatively, composite dikes, such as in Figs. 9 and 10. When there are chilled selvages (glassy margins) at the contacts between the rows, then the earlier row must have cooled down to a temperature similar to that of the host rock (the ambient temperature) before the next magma injection occurred. Thus, chilled selvages at the contact between the rows imply that the injections were separated by considerable time (at least tens or hundreds of years).

While earlier dikes generally encourage the injection of later dike-segments along the same path, an earlier dike may contribute to the formation of a stress barrier (due to dike-induced horizontal compressive stress) that tends to deflect a dike into a sill (Fig. 13) or stop the dike's vertical propagation altogether. For example, the sill in Fig. 17 was partly the result of a stress barrier generated by the composite dike in Fig. 9 (Gudmundsson, 2011b, 2020). Major dike-related stress barriers that generate sills, or arrest later dikes, however, tend to be created by thick dikes rather than, the more common, thin dikes (Gudmundsson, 2020). Also, even if stress barriers exist, often unrelated to earlier dikes, the later injected dike-segments commonly find a path that avoids the barrier so as to propagate to shallower crustal levels and, sometimes, to the surface (Fig. 22). This latter scenario happened in the eruptions in the Fagradalsfjall Volcanic System in Southwest Iceland in 2021, 2022, and 2023 (cf. Hobe et al., 2025).

A dike-related stress barrier, so that the (normally) maximum principal compressive stress is horizontal in the layer/unit that constitutes the barrier, is normally not a permanent feature in volcanic rift zones because crustal movements relax the compressive stresses over time. Most volcanic zones and volcanoes are subject to some sort of spreading, either due to gravity effects or through being located at plate boundaries. The spreading gradually relaxes the horizontal compressive stresses that earlier dikes may have induced, making it possible for later dikes again to use the margins or centres of earlier dikes as potential paths. The relaxation in horizontal dike-induced compressive stress (in a stress barrier) is especially noticeable at divergent plate boundaries. In particular, there are numerous examples of multiple dikes feeding eruptions – indicating that any dike-induced horizontal compressive stress had relaxed by the time of the later dike-segment injection – a topic to which we turn now.

7. Eruptions fed by multiple dikes

We have seen that many dikes, and in some fossil volcanic system the majority of the thicker dikes, are composed of several columnar rows

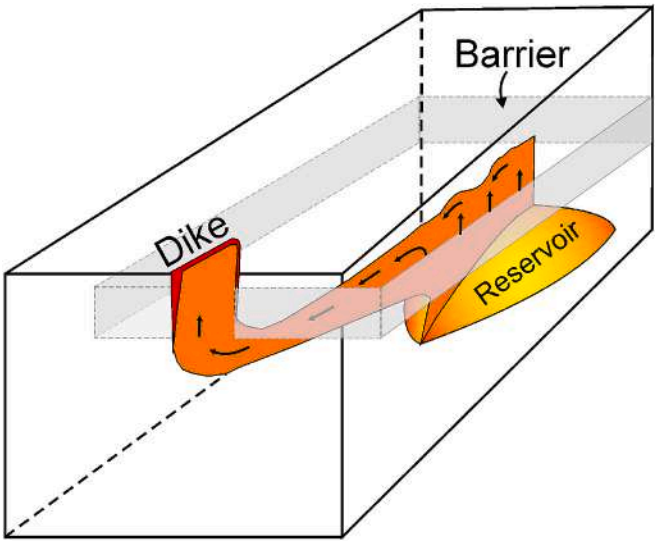

Fig. 22. Likely propagation path of a regional dike injected from a deep-seated reservoir (Fig. 4) that meets a major stress barrier (or an elastic mismatch) at a shallow depth where the vertical dike propagation becomes arrested. For a dike that continues to receive magma after the arrest of its vertical propagation, lateral propagation of the dike beneath the barrier is likely. Eventually, part of the dike may reach the surface (and erupt) along a path outside the stress barrier, in which case the length (strike-dimension) of the feeder (the volcanic fissure at the surface) is normally a small fraction of total length of the dike beneath the barrier. This conceptual model, proposed by Gudmundsson (1990), is supported by the actual course of events during the 2021 dike emplacement and eruption in Fagradalsfjall in Southwest Iceland.

that reflect many magma injections along essentially the same dike path. Such dikes are traditionally named multiple if all the rows of columns are composed of the same or similar lithology (say basalt) and composite if some of the rows are of widely different lithology (say rhyolite rows alternating with basaltic rows). I have also provided evidence for a compose dike feeding an old composite lava flow (Fig. 10; Gibson and Walker, 1963). But what is the evidence for multiple dikes feeding recent and well-documented eruptions?

Examples of dikes using existing earlier dikes at paths to the surface to feed eruptions are numerous. Here I first discuss briefly some examples from Etna and Kilauea and then in greater detail some specific and well-documented examples from Iceland.

7.1. Etna, Italy

One comparatively recent case of a multiple feeder-dike was reported from the Etna Volcano, Italy, in 2013. The data on the dike formation were obtained mainly through monitoring the surface fracturing above (primarily) laterally propagating dike-segments at very shallow depths. During the formation of the dike, Falsaperla and Neri (2015) estimated the velocity of magma injections as being from 0.02 m s^{-1} to as high as 0.46 m s^{-1}. The high velocity, however, was recorded for the later dike-segment injections that were partly along the earlier dike-segment injections during the same episode. Thus, the later injected dike-segments or magma injections propagated at a higher rate because the propagation was easier along the already formed earlier dike-segments – in accordance with the theory of least action/minimum potential energy proposed here.

7.2. Kilauea, Hawaii, USA

In the Kilauea Volcano in Hawaii the very high rate of migration of some earthquake swarms, interpreted as primarily lateral propagation of magma or dike-segment injections, varies by over four orders of magnitude. More specifically, the inferred lateral dike-segment propagation migration down the rift has been from 0.005 m s^{-1} to 8.5 m s^{-1} (Rutherford and Gardner, 2000). Many dike-segments have supplied magma to eruptions. The high velocities are likely to involve multiple dikes where the later dike injections propagated rapidly along the already existing dike path, using either the hot centre of the previously injected dike or the earlier dike contact with the host rock. As is observed, and in agreement with the theory presented here, there is no difference in the propagation rates of feeder and non-feeder dikes.

During the caldera collapse in 2018 that marked the end of the more-or-less continuous eruption in Kilauea since 1983 (so for about 35 years) magma was injected primarily laterally into the rift zone from the chamber below the caldera. During that collapse even higher lateral velocities were reported than those listed by Rutherford and Gardner (2000). The 2018 Kilauea collapse occurred in 62 ring-fault slips over a period of about 3 months (Neal et al., 2019). During each slip and associated magma-chamber volume reduction, a 'pressure pulse' is thought to have travelled in 13–20 min a distance of about 40 km along the feeder-dike to the erupting fissure, where the effusion rate thereby temporarily increased. However, while there was a noticeable increase in effusion rate from the fissure 13–20 min after the each fault slip, the peak in effusion following each caldera slip was observed some 2–4 h later. Thus, whereas the pressure 'pulse' travelled along the feeder-dike at the rate of about 40 m s^{-1}, the main effects of the pressure 'disturbance' as reflected in the peak effusion rate travelled at a rate of about 4 m s^{-1} from the chamber to the erupting volcanic fissure. At its maximum the effusion rate increased from an average pre-slip rate of 153 m^3s^{-1} to 400–500 m^3s^{-1} (Patrick et al., 2019).

These observations suggest that the magma injections following each caldera slip were multiple injections that were mostly confined to, and following, the already existing feeder-dike. The pressure 'pulses' at 40 m s^{-1}, however, are unlikely to reflect lateral migration rates of the magma injections (the dike-segments) themselves, but rather the rate of travel of pressure disturbances – as waves - along the magma in an already existing feeder-dike. By contrast, the propagation rate of 4 m s^{-1}, even if high, may reflect the actual velocity of the movement of new magma injections along the multiple feeder-dike.

7.3. Hekla, Iceland

Hekla is a central volcano, a stratovolcano, located in South Iceland, more specifically in the East Volcanic Zone (Fig. 23). The volcano forms an elongated volcanic ridge that reaches an elevation of 1480 m a.s.l. and has a clear 5.5-km-long summit fissure where most of the proper Hekla eruptions take place. The repeated eruptions in the same fissure are fed by a multiple dike. Hekla forms the central part of the Hekla Volcanic System, whose length and width are variously estimated as 40 km and 7 km, respectively (Jakobsson, 1979) or 60 km and 19 km (Thordarson and Hoskuldsson, 2008). The Hekla Volcanic System has produced basalts, basaltic andesites, andesites, and dacites-rhyolites.

The volcanic fissures and tectonic fractures in the East Volcanic Zone in the vicinity of Hekla strike mostly N40–45°E, and yet the summit fissure, and the elongated ridge of Hekla itself, strikes N65°E (Gudmundsson and Brenner, 2003). The strike of the summit fissure of Hekla coincides with the general strike of the sinistral faults of the South Iceland Seismic Zone (SISZ). Consequently, Gudmundsson and Brenner (2003) proposed that the summit fissure of Hekla was initially an ENE-trending sinistral fault of the SISZ. In that model, accumulation of tensile, and partly shear, stresses in the transtension quadrant where Hekla is located (Figs. 23, 24) contributes to the formation of the multiple feeder-dike and associated eruptions of Hekla.

Hekla is among the most active central volcanoes in Iceland both as regards production of lava and tephra and frequency of eruptions. During historical time in Iceland, the past 1100 years since the settlement, at least 18 eruptions have occurred in Hekla itself, and 4–5 in its immediate vicinity (Thordarson and Larsen, 2007). The most recent eruption was in the year 2000. This means that a feeder-dike reaches the summit fissure to erupt on average once every 60 years. The measured crustal dilation across the southern part of the East Volcanic Zone (EVZ), where Hekla is located (Fig. 23), is 11 mm per year (Arnadottir et al., 2008). This dilation/spreading is divided among 5–6 volcanic systems (Fig. 23; Arnadottir et al., 2008). On average, the spreading is about 2

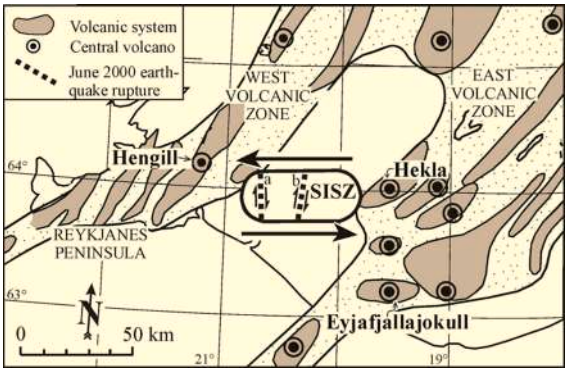

Fig. 23. Hekla Volcano is located in the northeast quadrant of the South Iceland Seismic Zone (SISZ). Because of the overall sinistral movements across the SISZ, Hekla is located in a region of tension which contributes to the same dike path opening up again and again in the eruptions of Hekla, namely the Hekla Fissure, thereby generating a multiple dike. By contrast, other central (composite) volcanoes close to the SISZ, such as Hengill and Eyjafjallajokull, are located in regions of compression. There is no central volcano in the southwest quadrant (Fig. 24). Also shown are N-S-striking dextral faults (a, b) which, together with the conjugate ENE-striking sinistral faults (one presently forming the Hekla Fissure), are common in the SISZ (modified from Gudmundsson and Brenner, 2003).

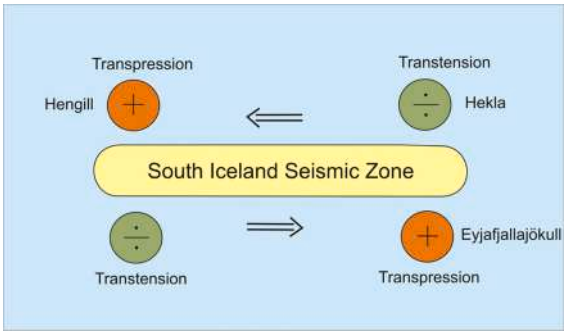

Fig. 24. Sinistral displacement across the SISZ results in the Hekla Volcano concentrating relative tensile stresses (Hekla is in a quadrant of transtension), whereas the volcanoes Hengill and Eyjafjallajökull concentrate compressive stresses (are in a quadrants of transpression). The tensile stress concentration at the Hekla Volcano results in the same fissure (an old ENE-striking sinistral fault) being reactivated again and again during eruptions, resulting in the formation of a multiple dike.

mm per year per volcanic system. This yields a spreading in the Hekla System over 1100 years of about 2.2 m (2200 mm) and for the Holocene (11,700 years) about 23 m.

The spreading-rate estimates are based on GPS measurements over a few decades and the fraction of the spreading taken up by the Hekla Volcanic System is not known in detail. Additionally, because of the strike of the summit fissure of Hekla in relation to the orientation of the spreading vector there will not only be opening across the summit fissure but also shear. The shearing is also implied in the suggestion (Gudmundsson and Brenner, 2003) that the Hekla is a reactivated sinistral strike-slip fault. These crude spreading estimates show, however, that there is significant spreading-generated 'space' for a multiple dike to form over a long period of time in Hekla.

The source magma chamber of Hekla has been difficult to detect. For example, recent estimates put the depth to the top of the chamber/reservoir somewhere between 5 km and 24 km (Geirsson et al., 2012). Whatever the exact depth to the Hekla chamber/reservoir, it has been difficult to explain in the past decades how little, shallow, and of short duration the earthquake activity is before the eruptions of Hekla.

The multiple-dike model of Hekla's eruption can be used to explain the shallow/little/short-time warning of earthquakes before eruptions. Because of the existing path along the multiple dike that already extends to the surface, there is little energy and little rupturing (Eqs. 12–15) needed to propagate a new dike-segment to the surface. While some earthquakes would occur in the walls of the path simply because of the added magmatic pressure, which results in slip on existing fractures in the host rock of the multiple dike (Gudmundsson, 2020, 2022), very little rupturing of the host rock occurs because the path is already there along the existing dike. The only rupturing is likely to occur at the shallow depths along the dike path, where the earlier dike-segment injections have not only solidified but already reached a temperature similar to that of the host rock. At greater depths the most recent dike-segment is still hot even if solidified, and in some cases very hot and with plastic/ductile behaviour at great depths. This applies particularly during the past decades when the repose period (the time between eruptions) of Hekla has been much shorter than the average.

In the past 1100 years (historical time in Iceland), the repose of Hekla has varied from 9 years to 120 years. The shortest period, the one preceding the 2000 eruption, was only 9 years. The repose periods prior to the 1980 and 1991 eruptions were also unusually short, about a decade. When the repose period is so short, the deeper segments of the most recent parts of the multiple dike are still hot so that the path for the new magma injection/dike-segment forms easily without much rupturing and earthquakes.

The unusually short repose periods prior to the most recent eruptions may also be partly related to tensile (and shear) stress concentrations around Hekla in response to loading of the SISZ to failure. In terms of this model (Gudmundsson and Brenner, 2003) loading of the SISZ and associated tensile (and shear) stresses in the Hekla System contribute to frequent eruptions in Hekla primarily if the summit fissure (and its extension down to the source magma reservoir) is already occupied by a recently injected dike, the deeper parts of which are still hot, that concentrates stresses at its contacts with earlier dikes and with the host rock. Such a dike was provided by the 1970 Hekla eruption. Furthermore, the stress concentration and associated dike injections and eruptions in the Hekla depend on the seismic cycle. Thus, the February 2000 eruption in Hekla occurred before the June 2000 earthquakes in the SISZ (Fig. 23). These earthquakes reached M6.6 and relaxed part of the accumulated stress in the SISZ and, therefore, the stress concentration in its surrounding areas such as in the quadrant where Hekla is located (Figs. 23 and 24). There is thus, presumably, less tensile stress concentration currently in and around Hekla than was before the eruptions of 1980–81, 1991, and 2000. The conditions of a new magma injection and addition to the multiple feeder-dike in Hekla have, therefore, not been satisfied now for over two decades.

7.4. *Krafla, Iceland*

We now come to a special type of volcanic activity that in Iceland is referred to as 'fires'. These include the recent Krafla Fires (1975–84), the Fagradalsfjall Fires (2021−23) and the current Sundhnukur Fires (since 2023). 'Fires' of this kind refer to many volcanic eruptions, over years or decades, within the same volcano or volcanic system. Not all the eruptions in fires need occur at exactly the same location, the same volcanic fissure, but normally all the eruptions occur within a narrow zone in the same volcano/volcanic system. Here I propose that all such fires are fed by multiple dikes, and that the dike-segment that eventually reaches the surface as a volcanic fissure during each eruption in the fires is but a small part of the total length of the multiple feeder-dike. The location of the volcanic fissures varies during the fires, depending on where, exactly, each small dike-segment propagating from the main multiple dike at depth finds its way to the surface.

There is clear evidence for the formation of a multiple dike during the Krafla Fires in North Iceland in the period from 1975 to 1984. During this period there were at least 21 dike-segment injections, 9 of which reached the surface to feed eruptions (Tryggvason, 1977, 1983, 1984). In the course of the 9-year rifting episode, much of the 100 km long and 4–10 km wide Krafla Volcanic System (Figs. 25, 26) was subject to volcanotectonic events. These included, in addition to the the 21 dike-segment injections, subsidence of the central part and rise of the flanks of the volcanic system (which includes several shallow grabens), as well as fracture development and crustal dilation.

The growth of the multiple feeder-dike responsible for the 9 eruptions can be inferred from the measured crustal dilation in an 18-km-long profile from the mountain Hlidarfjall in the south to the mountain Hrutafjöll (Figs. 25, 27). This is because the feeder-dike segments of all the 9 fissure eruptions occurred within 7 km of the Krafla caldera fault (Fig. 26). The crustal dilation in this part of the volcanic system, namely where the fissure eruptions occurred, was measured more accurately than in other parts of the volcanic system.

The results as to the growth of the multiple feeder-dike during the 9 eruptions can be inferred from the associated crustal dilation (Fig. 27). The total length of resulting discontinuous volcanic fissure is 11 km (Saemundsson, 1991) while the length of the measurement profile is 18 km and thus extends well beyond the fissure, both in the south and in the north. The volcanic fissures were short in the early eruptions, but generally longer in the later eruptions, with the total lengths of the discontinuous fissures in the last two eruptions (in 1981 and 1984) of 8–9 km (Saemundsson, 1991). Not only did the fissures in the later eruptions commonly coincide with those from the earlier eruptions, but some of the fissures also coincided with the fissure formed in 1729, that

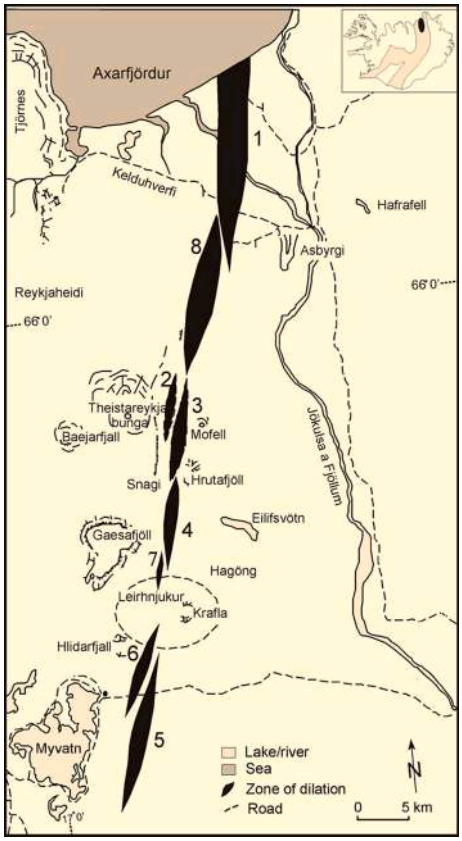

Fig. 25. Dike injection and rifting occurred in the Krafla Volcanic System from 1975 to 1984. The main rifting occurred where the dike reached shallow depths. In 9 dike injections, out of at least 21, part of the dike reached the surface to feed an eruption. Here is a schematic illustration of the size and location of the areas (black) where the main rifting/surface fracturing occurred during 8 dike injections from 1975 to early 1978. The numbers indicate the order, so that number 1 is the oldest and number 8 the youngest dike injection/rifting event during this period. No surface fracturing, however, was observed during two dike injections during this period. Modified from Sigurdssson (1977) and Gudmundsson (1995a).

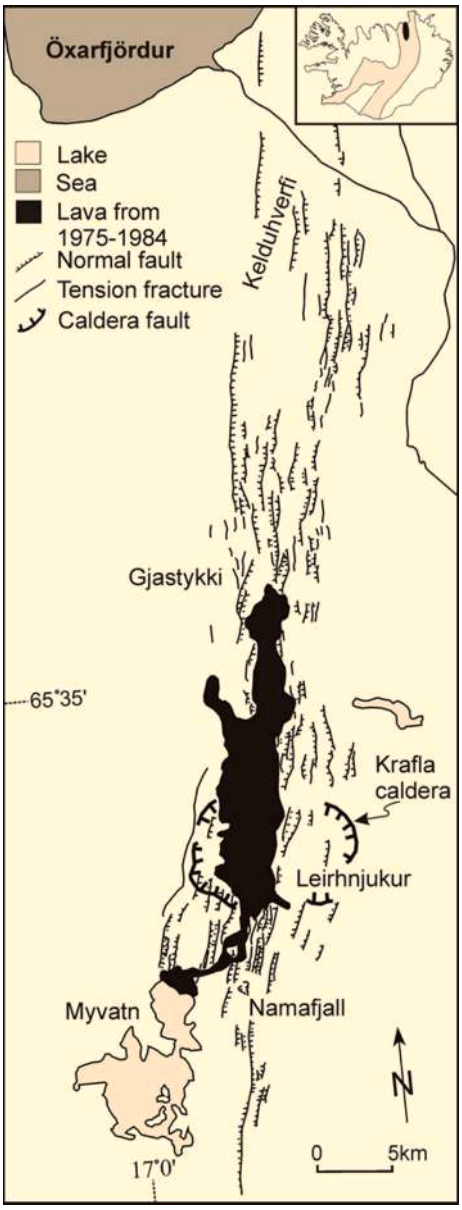

Fig. 26. Main volcanotectonic elements of the Krafla Volcanic System. Indicated are the Krafla Caldera, the hill Leirhnjukur, which was the centre of the inflation and deflation associated with the magma chamber expansion, rupture, and dike-segment injection during the multiple dike formation (Fig. 27), the fissure swarm and lava flows. The basaltic lava flows formed mostly during the Krafla fires, 1975 to 1984, but also in the Myvatn fires, 1724 to 1729 (whose feeder-dike also forms part of the multiple dike). On the inset of Iceland, the active volcanic zone is shaded. Modified from Gudmundsson (1995a).

is, some 250 years earlier, during earlier fires (so-called Myvatn Fires, from 1724 to 1729; Saemundsson, 1991) in the Krafla Volcanic System. The length and thickness of the feeder-dike thus gradually increased during the Krafla Fires.

While some of the measured crustal dilation profiles represent more than one feeder-dike segment injections, the profiles associated with the 8th and 9th eruptions reflect the dilation due to single dike-segment injections (Fig. 27). Both indicate a close-to ideal dike-opening displacement, namely a flat ellipse (Gudmundsson, 1995a, 2011a), 12–15 km long with total fissure length at the surface of 8–9 km. The maximum dilation for both profiles is about 1 m and located approximately in the centre of the profile. Because the geodetic (levelling) measurements were made at a distance from the feeder-dike, its thickness is presumably somewhat over one metre.

All the 9 volcanic fissures associated with the feeder-dike injections were discontinuous and offset in lateral sections. The beginning of each eruption was on a short fissure segment, but subsequently other segments formed as further dike 'fingers' reached the surface. This is normal in fissure eruptions and widely observed, such as in the recent eruptions on the Reykjanes Peninsula (Section 7.5). From their initiation, the short segments propagated laterally, that is, increased their lengths at the rate of 0.1–0.4 m s^{-1} (Tryggvason, 1977; Gudmundsson, 1995a). Based on the total length of the fissures of 11 km and the maximum thickness of the multiple feeder-dike of about 9 m (Fig. 27), the length/thickness or aspect ratio of the multiple dike is about 1200 – similar to that of many regional dikes in Iceland (Gudmundsson, 2020).

The Krafla Volcanic System is in the North Volcanic Zone. It is thus of interest to compare the multiple feeder-dike formed in the Krafla Fires with exposed dikes in the nearby fossil volcanic systems. Hundreds of (mostly basaltic) dikes have been studied in the nearby fossil systems, of Neogene age, on the peninsulas of Flateyjarskagi and Tröllaskagi (Gudmundsson, 1995b). The mode thickness of dikes in these swarms is about 1 m, that is similar to the individual dike-segment injections in the multiple feeder-dike formed during the Krafla Fires. Additionally, multiple dikes are very common in the fossil systems, with many dikes reaching thicknesses of 6–20 m (Figs. 1, 8, 9, 11, 12) and occasionally as thick as many tens of metres (Fig. 14). Thus, the observed feeder-dike

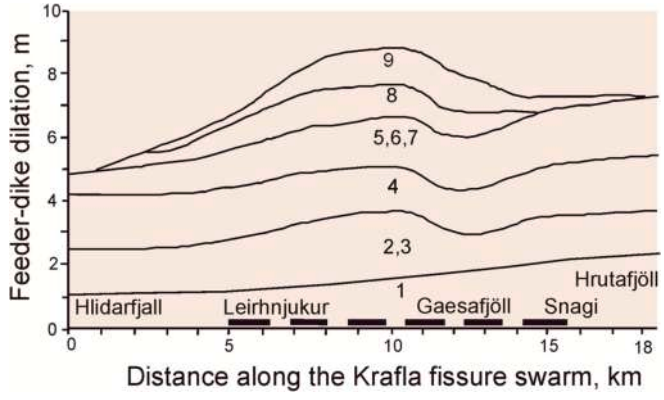

Fig. 27. Growth of the multiple feeder-dike during the 9 eruptions in the Krafla Volcanic System from 1975 to 1984. The 18-km-long crustal dilation profile extends to the south and to the north of the Krafla Caldera (Figs. 25, 26). The broken lines between Leirhjukur and Snagi parallel with the horizontal axis of the diagram shows the final length of the volcanic fissure, whose segments were longer in the later eruptions, indicating an increase in the length of the associated feeder-dike segment (columnar row). In some of the early eruptions, the measured crustal dilation was the cumulative dilation due to two or three dike injections, but the 8th and the 9th eruption represent only a single dike injection. The thickness increase during each dike injection was about 1 m, in good agreement with the common thicknesses of single columnar rows in regional basaltic dikes in Iceland (Figs. 1, 11). The final length of feeder-dike at the surface was 11 km and its maximum thickness about 9 m, in good agreement with typical length/thickness ratios of regional basaltic dikes in Iceland (Gudmundsson, 2020). Data from Eysteinn Tryggvason (cf. Tryggvason, 1977, 1983, 1984).

emplacement in the Krafla Fires is in harmony with what is observed in nearby fossil Neogene volcanic systems in North Iceland.

7.5. Fagradalsfjall and Sundhnukur, Iceland

Fagradalsfjall is a volcano located on the Reykjanes Peninsula in Southwest Iceland (Fig. 28; Troll et al., 2024; Hobe et al., 2025). The volcano erupted in 2021, 2022, and 2023 (Fig. 29). The 2021 eruption was the first one to occur on the Reykjanes Peninsula in 781 years, and the first one in Fagradalsfjall in about 8000 years. Using seismic

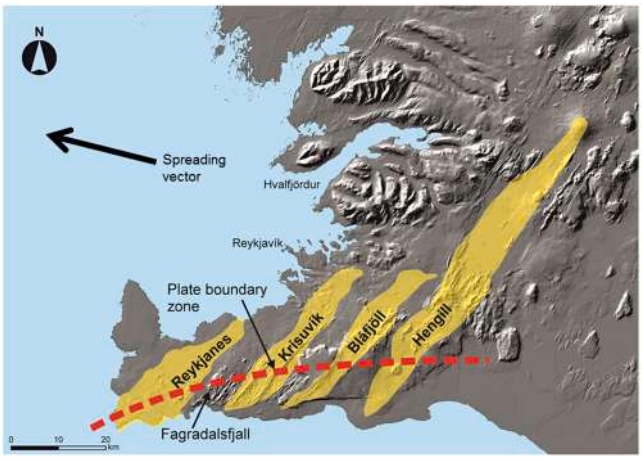

Fig. 28. Location and geometry of the main volcanic systems on the Reykjanes Peninsula in relation to the location of the volcano Fagradalsfjall (to the west of which is Sundhnukur, Fig. 29) where the multiple dike-fed eruptions of 2021, 2022 and 2023 occurred. Also shown are the plate-boundary zone, where the main strike-slip seismic activity associated with plate movements on the peninsula takes place, and the orientation of the spreading vector. The volcanic systems are Reykjanes, Krisuvik, Blafjöll, and Hengill.

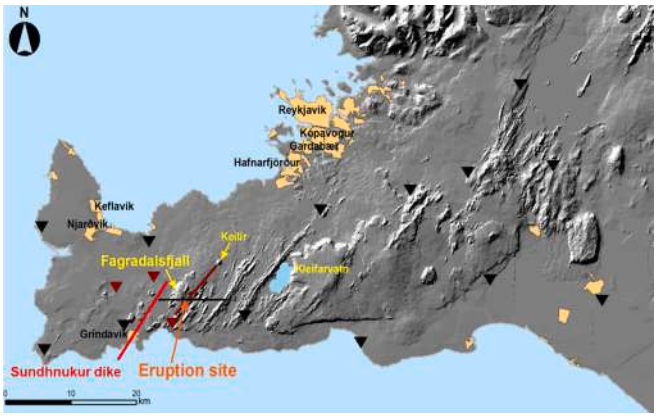

Fig. 29. Location of the 9-km-long multiple dike that formed in the Fagradalsfjall eruptions of 2021–2023, (dark red) and the 15-km-long multiple dike formed in the Sundhnukur eruptions 2023–2024 (light red). Orientation and maximum strike-dimension (length) are here shown for the 2021 eruption (red NE-trending line), but the subsequent dike injection were at similar locations. The dike length (strike-dimension) shown here is the maximum length, of about 9 km, not the length of the feeder (the volcanic fissure) at the surface, which was only a few hundred metres in each of the 3 eruptions. Thus, for the most part the multiple dike formed from 2021 to 2023 became arrested, at about 2 km depth below the surface, and only a small 'finger' reached the surface in each of the eruptions. The depth (dip-dimension) of the part of the multiple dike that became a feeder, that is, the depth to the source reservoir, is 9–10 km. Also indicated are the eruption site, the hyaloclastite mountain Keilir, Lake Kleifarvatn, the employed seismic network (red triangles), the SIL seismic network stations (black triangles), the profile (black E-W trending (horizontal) line dissecting the dike) for the tomographic results presented by Hobe et al. (2025). The urban areas of Grindavik, Njarðvik, Keflavik, Hafnarfjördur, Gardabær, and Kopavogur and Reykjavik are shown. (For interpretation of the references to colour in this figure legend, the reader is referred to the web version of this article.)

methods, a deep-seated reservoir with the shallowest depth of the roof at about 10 km depth below the surface was identified (Hobe et al., 2025). The dike injections in 2021, 2022 and 2023 occurred when the roof of this reservoir ruptured. The source of all these magma injections is thus a deep-seated reservoir, located close to the contact between the upper mantle and the lower crust. In fact, neither Fagradalsfjall nor other volcanic systems on the Reykjanes Peninsula have a long-lived shallow crustal magma chamber. They are all fed by deep-seated reservoirs located in the lower crust or at the boundary between the crust and the upper mantle (Gudmundsson, 2006, 2020). It follows that the injected dike-segments propagated initially primarily vertically, in a direction towards the surface.

Through the analysis of associated earthquakes, the rupture of the reservoir and the initiation of dike-segments that eventually fed the 2021 eruption could be determined very accurately. The main rupture and dike-segment injection occurred on 24 February and then there was second major dike-segment injection on 15 March. The first dike-segment injection propagated vertically up do a depth of, mostly, 2 km below the surface. There this segment became vertically arrested at a stress barrier. Since it continued to receive magma it propagated laterally under the barrier (Fig. 22). The lateral propagation was initially to the northeast and subsequently to the southwest, eventually resulting in a maximum dike length of about 9 km (Hobe et al., 2025).

The second main dike-segment injection, namely on 15 March, also resulted in dike-segment propagation (Hobe et al., 2025). The injected second dike-segment generated partly its own path but partly followed the path of the earlier-injected dike-segment – the one injected on 24 February. Thus, the second segment combined with the first one to form a multiple dike – similar in thickness to the columnar rows seen in Figs. 1, 11, 12, and 20. Part of the multiple dike eventually reached the

surface, as a 'tiny finger' generating, initially, a 180-m-long volcanic fissure at the surface on 19 March. The opening, or dike thickness, at the surface, however, was only about 0.2 m. This means that the feeder-segment that reached the surface had a thickness similar to that seen in Figs. 3 and 13. The fissure gradually became longer, with additional segments forming, but the fissure-segments remained disconnected and offset, and the total length, at its maximum, was only several hundred metres. Most of the 9-km-long multiple dike emplaced primarily as a result of the two dike-segment injections and propagation from 24 February to 19 March did not reach the surface to feed the eruption but rather became arrested mainly at about 2 km depth. The 2021 eruption lasted until 18 September 2021 or about 6 months.

An earthquake swarm began again in Fagradalsfjall on 30 July 2022, resulting in dike-segment injection and propagation. Some 10,000 earthquakes were recorded prior to the eruption, or about ¼ of the number recorded before the 2021 eruption. The reason for the fewer earthquakes is that in this case the propagation to the surface was easier for the dike than in 2021 because the 2021 multiple dike already existed. The dike-fed eruption began on 3 August. The initial fissure was about 300 m long, but the eruption lasted only for 18 days, ending on 21 August. The 2022 dike-segment also followed partly the segments injected in 2021, thereby adding a segment or row to the existing multiple dike. Thus, the new dike-segment propagated from the source reservoir to the surface in much shorter time than in the 2021 eruption, or in 3–4 days. For comparison, the first dike-segment in 2021 became permanently arrested and never made it to the surface. However, the second dike-segment of 2021, the one injected on 15 March, made it to the surface, partly along the existing first dike-segment, in about 5 days, so similar to the time that it took the dike-segment to reach the surface in the 2022 eruption.

The third eruption in the Fagradalsfjall in as many years occurred on 10 July 2023. The eruption was preceded by an earthquake swarm which initiated on 4 July. The recorded earthquakes were similar in number (about 12,000) and intensity as in the swarm occurring before the 2022 eruption. The reason for fewer earthquakes and less intense swarm than prior to the 2021 eruption is, as in the 2022 eruption, that a multiple dike already existed. The feeder-dike followed partly the same path as the dike injections in the eruptions of 2021 and 2022 to a shallow depth where, again, the dike-segment became arrested for a while. The first fissure to form was about 200 m long, or very similar to the first fissure that was generated in the 2021 eruption. Gradually the 2023 fissure grew laterally, but in an offset and an echelon manner. The volcanic fissures from 2021, 2022, and 2023 are not collinear but somewhat offset laterally, as is very common for volcanic fissures as well as dikes observed in the field. The location of all the feeder-dike segments at depth, however, indicates that there the paths to a large degree coincide so as to form a multiple dike.

The results from the Fagradalsfjall eruptions in 2021, 2022, and 2023 demonstrate how multiple dikes make eruptions easier. The first dike-segment injected in February 2021 propagated for about two weeks (from 24 February and at least until 9 March) but was not able to reach the surface to feed an eruption. Instead, the dike-segment became arrested, mostly at a depth of 2 km below the surface. The second dike-segment, injected on 15 March, reached the surface in less than 5 days (4.7 days or 112 h). A part of its propagation was along the existing dike-segment, suggesting its forming a multiple dike greatly facilitated is propagation and made it possible for it to reach the surface. Similarly, the third dike-segment, the feeder to the August 2022 eruption, again partly followed and added to the existing multiple dike and reached the surface in 3–4 days. The same applies to the feeder-dike of the 2023 eruption – the dike-segment reached the surface in less than a week. Clearly, therefore, the existing multiple dike facilitated the propagation of the 2022 and 2023 dike-segments, part of which reached the surface to feed eruption.

From December 2023 to December 2024 there were 7 fissure eruptions at the crater row Sundhnukur (Fig. 29), just a few kilometres west of Fagradalsfjall (De Pascale et al., 2024; Troll et al., 2024; Iceland Meteorological Office, 2025). All the eruptions occurred close to, or coincided with, an existing volcanic fissure, namely the 2350-year-old Sundhnukur crater row (Jonsson, 1983). The crater row has a total length of 8.3 km and an average strike of about 37°. The crater row is composed of 27 discontinuous segments, varying in length from 36 m to 1.8 km, and in azimuth from 006° to 053° (Jenness and Clifton, 2009). Segmentation of this kind is a common feature of volcanic fissures, dikes, and rock fractures in general (Gudmundsson, 2011a).

On 10 November 2023, before the first eruption (on 18 December 2023), a 15-km-long regional dike (Fig. 29) was emplaced in alignment with the Sundhnukur crater row, but extending much further to the southwest than the crater row. The dike became arrested at about 0.5 km depth, so did not erupt, but there was formation and reactivation of tension fractures and normal faults, including graben subsidence, at the surface (De Pascale et al., 2024).

The 7 eruptions in 2023–24 have occurred at different parts of the Sunhnukur crater row, but all have been so close to the old craters that there is little doubt that the feeders to these eruptions, and the arrested 15-km-long dike from 10 November 2024 (Fig. 29), are all contributing to the formation of a multiple dike (Gudmundsson, 2024a). The present multiple-dike formation is primarily because of the existence of the 2350-year-old feeder-dike to the Sundhnukur crater row. Thus, in the Sundhnukur Fires we see a similar process of a multiple dike formation as in the Krafla Fires. In both cases, an existing older feeder-dike (about 250 years old in the Krafla Fires and about 2350 years old in the Sundhnukur Fires) acts as a path for many dike-segment injections during these fires. These and the results above indicate that, as regards energy transformed during dike propagation, multiple dikes make eruptions comparatively easy.

8. Discussion

Reliable forecasting of volcanic eruptions is one of the main goals of volcanology. So far, forecasts have rarely been successful (Gudmundsson et al., 2022). Given that most eruptions on Earth are supplied with magma through dikes (and inclined sheets), understanding how dikes make their paths and how, where, and when they are able to reach the surface is of fundamental importance in theoretical and applied volcanology.

Many and probably most injected dike-segments do not reach the surface. They become arrested (Figs. 2 and 3), that is, stop their vertical propagation at various depth in the crust. Commonly, the arrest is at or close to contacts between mechanically dissimilar layers (Gudmundsson, 2003, 2011b; Gudmundsson and Brenner, 2004, 2005; Gudmundsson and Philipp, 2006; Moran et al., 2011; Drymoni et al., 2020; Inskip et al., 2020; Corti et al., 2023). While dike arrest and deflection into sills has received considerable attention in the past decades (Gudmundsson, 2011b), the way that dikes select their paths has only recently become of major interest. The idea that dikes follow the paths of least work or least potential energy was set forth decades ago (Gudmundsson, 1984, 1986), yet it has been developed further only in the past few years (Gudmundsson, 2020, 2022). These developments indicate that, in general, dike (and inclined sheet) paths follow the principle of least action which, when the kinetic energy is of little importance (as is common during dike propagation), reduces to the principle of least work or minimum potential energy - in agreement with observations of actual dike paths in the field (Gudmundsson, 2022).

A similar method of analysing and forecasting fracture propagation in general has become of great interest in recent years. This method is the variational approach to fracture (Bourdin and Francfort, 2008; Del Piero, 2013), a generalisation of Griffith's theory, and commonly referred to as the phase-field modelling of fractures. Earlier different approaches were used to forecast fracture paths (e.g., Pook, 2012), but the phase-field approach is currently much used for analysing fracture propagation and paths in computational mechanics and fracture

mechanics and related fields.

Initially, there were few applications of the phase-field modelling to rock fractures, but now there are many such applications (Chen et al., 2020; Fei et al., 2021). The dike tip and dike thickness (aperture), both of which are of fundamental importance for actual dike propagation, however, are not easily presented by the diffusive damage-like ('smeared') zone of a given 'width', which is the common approach in phase-field modelling. This is partly because the dike thickness ('width'), or the aperture of the propagating magma-driven fracture, is highly variable. Also, the effects of mechanical layering in general, and that of existing faults in particular, are currently not so easily taken into account in phase-field modelling. At present, because of its use of 'damage' approximation for the fracture, the phase-field approach may be more suitable for modelling faults than for modelling dikes. There is, after all, a real damage zone (and a porous, 'damaged' core as well) in fault zones – although real fault propagation is, of course, very different from that of extension fractures such that of dikes and fluid-driven fractures.

One aspect of dike propagation that has not received much attention until now is the effect of multiple dikes in facilitating dike propagation to the surface, resulting in dike-fed eruptions. The results presented here indicate that multiple dikes make eruptions mechanically easy for two main reasons. First, an existing dike provides a potential path for new dike injections, either along the contacts between the dike and the host rock or along the contacts between columnar rows in the dike. This applies not only to dikes but also to inclined sheets (Browning and Gudmundsson, 2015; Thiele et al., 2021). Second, since the rock of a multiple dike has everywhere essentially the same mechanical properties, the dike rock tends to homogenise the stress field favourably, thereby facilitating further magma injections and propagation along the existing dike in accordance with the principle of least action/minimum potential energy.

When a volcano or a volcanic system enters an unrest period, there are several points to consider for increasing the likelihood of a successful prediction of an eruption. First, the conditions for and likely location of chamber/reservoir rupture need to be clear and applied to the particular unrest period. Often the inflation gives an indication of the likelihood of a rupture and dike injection. The existence of a multiple dike dissecting the roof of the chamber usually increases the chance of magma-chamber rupture for a given excess pressure. However, the main evidence for magma-chamber rupture and dike injection is provided by earthquakes. In particular, a comparatively large earthquake in the roof of the chamber followed by a migrating earthquake swarm is normally a clear indication of chamber-roof rupture and dike injection. Often the location of the rupture can be determined reasonably accurately (Gudmundsson et al., 2022; Hobe et al., 2025).

Second, using the present theoretical framework whereby dikes are likely to follow the path of least action or, more specifically, the path of minimum potential energy, numerical models are of great help to forecast likely dike paths. Many such models that take into account the mechanical layering of volcanoes and volcanic systems have already been made (Gudmundsson, 2006, 2020). However, so far the effects of faults on potential dike paths have received less, albeit some, attention (Drymoni et al., 2020; Gudmundsson, 2022). More work in the direction of numerical modelling of dike propagation in layered and faulted volcanoes and volcanic systems will be of great value for reliable dike-path forecasting and is expected in the near future.

Increased and improved seismic and geological mapping of active volcanoes, particularly the most dangerous ones, are likely to result in gradually better knowledge of their internal structures. This knowledge, together with that of the effects of multiple dikes, should make it possible to provide more accurate numerical models as to the local stresses and likely paths of dikes within the volcanoes.

The main theme of this paper is that development of multiple dikes makes eruptions much more likely during magma-chamber/reservoir rupture and dike injection in a volcano/volcanic system. As the results from Krafla and Sundhnukur show, the multiple dike may be partly formed in a rapid succession of dike-injections over some years, and partly over periods of hundreds or thousands of years. It is suggested that multiple dikes stress-homogenise the potential path to the surface so as, commonly, to favour new dike injections reaching the surface. The homogenisation minimises the variation in the orientations of the local principal stresses generated by mechanically dissimilar rock layers or units along potential paths of dikes. Stress-homogenisation is presumably a necessary condition for generating major non-stratabound fractures, that is, fractures that dissect many layers/strata rather than being confined to a single layer/stratum. All feeder-dikes are non-stratabound fractures. The mechanism of stress-homogenisation is not confined to dike injections; it is commonly reached through faulting, as was discussed earlier (Gudmundsson and Homberg, 1999; Gudmundsson and Brenner, 2004, 2005; Gudmundsson, 2006; Gudmundsson et al., 2010) and in great detail in a recent publication (Gudmundsson, 2024b). In the present paper, however, the focus is on stress-homogenisation through dike injections. In volcanoes and volcanic zones composed of layers with widely different mechanical properties, stress-homogenisation - resulting in σ_1 in all the layers along the potential path being close to or actually vertical - is needed in order for dikes to have the chance of propagation to the surface, that is, to become feeder-dikes.

9. Summary and conclusions

This paper introduces the idea that multiple dikes – dikes formed by repeated injections of magma along the same path – increase the likelihood (in comparison with single-injection dikes) of dike-fed eruptions during unrest periods with magma-chamber/reservoir rupture. There are many examples of eruptions fed by multiple dikes worldwide. In the paper the focus is on some well-known volcanoes/volcanic systems where multiple dikes have supplied magma to eruptions. These are Etna in Italy, Kilauea in Hawaii, and Krafla, Hekla, Fagradalsfjall and Sundhnukur in Iceland. Further work in this direction will no doubt reveal many more examples of volcanoes supplied with magma through multiple dikes.

The main conclusions of the paper may be summarised as follows.

- Dikes (inclined sheets are here included) supply magma to most eruptions on Earth. Successful forecasting of volcanic eruptions in general therefore depends primarily on understanding of how dikes select their propagation paths following magma-source rupture and dike injection. That understanding must be based on knowing the physical principles that control dike-path selection and, in particular, the conditions for dike arrest.
- Many and perhaps most injected dike-segments become arrested. Some segments become totally arrested, that is, no part of the segment reaches the surface. For other segments, a fraction of its length may reach the surface, sometimes as a tiny 'finger' whose strike-dimension (horizontal length) is a small fraction of the total maximum strike-dimension of the dike at depth in the crust. Reliable assessment of the probability of dike arrest is thus of fundamental importance in volcanic hazard studies.
- Theoretical and observational results, summarised here, suggest that dike-segments (or dike-parts) select the paths based on Hamilton's principle of least (minimum) action. This implies that, among all possible paths, the one selected by a propagating dike-segment is the path along which the energy transformed (or released) multiplied by the time taken for the dike-segment propagation from its source to the surface (for a feeder) or point (or line) of arrest (for a non-feeder) is minimum. When the kinetic energy can be ignored (because dike propagating is comparatively slow), the Hamilton's principle implies that the dike-segment path chosen is the one that minimises the potential energy.
- Multiple dikes are dikes where two or more segments have been injected partly, or entirely, along the same path - commonly forming,

on solidification, columnar rows. The term multiple refers to dikes where all the parts (the columnar rows) are of essentially the same composition; for example, basalt. A multiple dike made of rocks of widely different composition, such as basalt and rhyolite, is referred to as composite. Multiple (and composite) dikes are very common in many fossil volcanic systems, such as in Iceland and parts of Scotland, and no doubt worldwide.

- Here I propose that multiple (and composite) dikes are common because they make dike propagation 'easier' (in comparison with the propagation of single dikes). By easier I mean that once a dike path has been established (through a dike injection), it normally requires less energy for subsequent dike injections to follow that path than to generate an entirely new path (a new single dike injection). This is because the first dike injection to a large degree stress-homogenises its path and, commonly, makes it favourable to subsequent dike injections. This means that there is much less chance of dike arrest or dike deflection into a sill when the subsequent dike-segment follows an existing path than if the segment forms its own path, particularly in volcanic systems and zones where the rock layers have widely different mechanical properties – conditions that normally favour dike arrest or deflection into a sill.
- Many active volcanoes and volcanic systems are fed by multiple dikes. This fact is best demonstrated through the monitoring of feeder-dikes. Many of those are known to follow the paths of earlier dikes, and thus to be multiple. The volcanoes fed partly by multiple dikes discussed here are Etna in Italy, Kilauea in Hawaii, and the Icelandic volcanoes Hekla, Krafla, Fagradalsfjall, and Sundhnukur. These all show clear evidence of some or most of their recent eruptions being fed by multiple dikes, thereby supporting the proposal in this paper that multiple dikes make eruptions easy.

CRediT authorship contribution statement

Agust Gudmundsson: Writing – review & editing, Writing – original draft, Investigation, Funding acquisition, Formal analysis, Data curation, Conceptualization.

Declaration of competing interest

The author declares that he has no known competing financial interests or personal relationships that could have appeared to influence the work reported in this paper.

Acknowledgements

The results presented in this paper are based on work over many years that was supported by several funding agencies. These include the Icelandic Science Foundation, the Research Council of Norway, the European Commission, and the Natural Environment Research Council of the United Kingdom. I thank the journal reviewers for very helpful comments.

Data availability

All the data relevant to the analysis of multiple dikes presented here are in the paper itself or in cited publications.

References

Agustsdottir, T., Woods, J., Greenfield, T., Green, R.G., White, R.S., Winder, T., Brandsdottir, B., Steinthorsson, S., Soosalu, H., 2016. Strike-slip faulting during the 2014 Bardarbunga-Holuhraun dike intrusion, Central Iceland. Geophys. Res. Lett. 43, 1495–1503.

Al Shehri, A., Gudmundsson, A., 2018. Modelling of surface stresses and fracturing during dyke emplacement: application to the 2009 episode at Harrat Lunayyir, Saudi Arabia. J. Volcanol. Geotherm. Res. 356, 278–303.

Anderson, T.L., 2005. Fracture Mechanics: Fundamentals and Applications, 3rd ed. Taylor & Francis, London.

Arnadottir, T., Geirsson, H., Jiang, W., 2008. Crustal deformation in Iceland: plate spreading and earthquake deformation. Jokull (The Icelandic Journal of Earth Sciences) 58, 59–74.

Bazargan, M., Gudmundsson, A., 2019. Dike-induced stresses and displacements in layered volcanic zones. J. Volcanol. Geotherm. Res. 384, 189–205.

Bazargan, M., Gudmundsson, A., 2020. Stresses and displacements in layered rocks induced by inclined (cone) sheets. J. Volcanol. Geotherm. Res. 401. https://doi.org/10.1016/j.jvolgeores.2020.106965.

Bedford, A., 1985. Hamilton's Principle in Continuum Mechanics. Pitman Publishing, London.

Bourdin, B., Francfort, G.A., Marigo, J-J., 2008. The Variational Approach to Fracture. Springer-Verlag, Berlin.

Browning, J., Gudmundsson, A., 2015. Caldera faults capture and deflect inclined sheets: an alternative mechanism of ring dike formation. Bull. Volcanol. 77, 1–13.

Browning, J., Drymoni, K., Gudmundsson, A., 2015. Forecasting magma-chamber rupture at Santorini volcano, Greece. Sci. Rep. 5, 15785. https://doi.org/10.1038/srep15785.

Chen, B., Sun, Y., Barboza, B.R., Barron, A.R., Li, C., 2020. Phase-field simulation of hydraulic fracturing with revised fluid model and hybrid solver. Eng. Fract. Mech. 229. https://doi.org/10.1016/j.engfracmech.2020.106928.

Corti, N., Bonali, F.L., Russo, E., Drymoni, K., Mariotto, F.P., Gudmundsson, A., Esposito, R., Cavallo, A., Tibaldi, A., 2023. Feeders vs arrested dikes: a case study from the Younger Stampar eruption in Iceland. J. Volcanol. Geotherm. Res. 443. https://doi.org/10.1016/j.jvolgeores.2023.107914.

Davis, R.J., Mathias, S.A., Moss, J., Hustoft, S., Newport, L., 2012. Hydraulic fractures: how far can they go? Mar. Pet. Geol. 37, 1–6.

De Pascale, G.P., Fischer, T.J., Hrubcova, W.M.P., et al., 2024. On the move: 2023 observations on real time graben formation, Grindavik, Iceland. Geophys. Res. Lett. 51, e2024GL110150. https://doi.org/10.1029/2024GL110150.

Del Piero, G., 2013. A Variational Approach to Fracture and Other Inelastic Phenomena. Springer-Verlag, Berlin.

Drymoni, K., Browning, J., Gudmundsson, A., 2020. Dyke-arrest scenarios in extensional regimes: insights from field observations and numerical models, Santorini, Greece. J. Volcanol. Geotherm. Res. 396. https://doi.org/10.1016/j.jvolgeores.2020.106854.

Dzurisin, D., 2006. Volcano Deformation: New Geodetic Monitoring Techniques. Springer Verlag, Berlin.

Elshaafi, A., Gudmundsson, A., 2016. Volcano-tectonics of the Al Haruj Volcanic Province, Central Libya. J. Volcanol. Geotherm. Res. 325, 189–202.

Emeleus, C.H., Bell, B.R., 2005. The Palaeogene Volcanic Districts of Scotland: Regional Geology Guide, 4th ed. British Geological Survey, Keyworth.

Falsaperla, S., Neri, M., 2015. Seismic footprints of shallow dyke propagation at Etna, Italy. Sci. Rep. 5, 11908. https://doi.org/10.1038/srep11908.

Fei, F., Choo, J., Liu, C., White, J.A., 2021. Phase-Field Modelling of Rock Fractures With Roughness. arXiv:2105, 14663v2.

Fisher, K., 2014. Hydraulic fracture growth: real data. In: Presentation given at GTW-AAPG/STGS Eagle Ford plus Adjacent Plays and Extensions Workshop, San Antonio, Texas, February 24-26, p. 2014.

Fisher, K., Warpinski, N., 2011. Hydraulic fracture-height growth: real data. In: Society of Petroleum Engineers Annual Technical Conference and Exhibition, SPE, 145949.

Flewelling, S.A., Tymchak, M.P., Warpinski, N., 2013. Hydraulic fracture height limits and fault interactions in tight oil and gas formations. Geophys. Res. Lett. 40, 3602–3606.

Fung, Y.C., Tong, P., 2001. Classical and Computational Solid Mechanics. World Scientific Publishing, Singapore.

Galindo, I., Gudmundsson, A., 2012. Basaltic feeder dykes in rift zones: geometry, emplacement, and effusion rates. Nat. Hazards Earth Syst. Sci. 12, 3683–3700.

Geirsson, H., LaFemina, P., Arnadottir, T., Sturkell, E., Sigmundsson, F., Travis, M., Schmidt, P., Lund, B., Hreinsdottir, S., Bennett, R., 2012. Volcano deformation at active plate boundaries: deep magma accumulation at Hekla volcano and plate boundary deformation in South Iceland. J. Geophys. Res. 117, B11409. https://doi.org/10.1029/2012JB009400.

Geshi, N., Neri, M., 2014. Dynamic feeder dyke systems in basaltic volcanoes: the exceptional example of the 1809 Etna eruption (Italy). Front. Earth Sci. 2. https://doi.org/10.3389/feart.2014.00013.

Geshi, N., Kusumoto, S., Gudmundsson, A., 2010. Geometric difference between non-feeder and feeder dikes. Geology 38, 195–198.

Geshi, N., Kusumoto, S., Gudmundsson, A., 2012. Effects of mechanical layering of host rocks on dike growth and arrest. J. Volcanol. Geotherm. Res. 223-224, 74–82.

Gibson, I.L., Walker, G.P.L., 1963. Some composite rhyolite/basalt lava flows and related composite dykes in eastern Iceland. Proc. Geol. Assoc. Lond. 74, 301–318.

Grandin, R., Jacques, E., Nercessian, A., et al., 2011. Seismicity during lateral dike propagation: insights from new data in the recent Manda Hararo–Dabbahu rifting episode (Afar, Ethiopia). Geochem. Geophys. Geosyst. 12. https://doi.org/10.1029/2010GC003434.

Gudmundsson, A., 1984. A Study of Dykes, Fissures, and Faults in Selected Areas of Iceland. PhD Thesis,. University of London.

Gudmundsson, A., 1986. Formation of dykes, feeder-dykes and the intrusion of dykes from magma chambers. Bull. Volcanol. 47, 537–550.

Gudmundsson, A., 1990. Emplacement of dikes, sills and crustal magma chambers at divergent plate boundaries. Tectonophysics 176, 257–275.

Gudmundsson, A., 1995a. The geometry and growth of dykes. In: Baer, G., Heimann, A., Balkema (Eds.), Physics and Chemistry of Dykes, Rotterdam, pp. 23–34.

Gudmundsson, A., 1995b. Infrastructure and mechanics of volcanic systems in Iceland. Tecctonophysics 64, 1–22.

Gudmundsson, A., 2003. Surface stresses associated with arrested dykes in rift zones. Bull. Volcanol. 65, 606–619.
Gudmundsson, A., 2006. How local stresses control magma-chamber ruptures, dyke injections, and eruptions in composite volcanoes. Earth Sci. Rev. 79, 1–31.
Gudmundsson, A., Simmenes, T.H., Larsen, B., Philipp, S.L., 2010. Effects of internal structure and local stresses on fracture propagation, deflection, and arrest in fault zones. J. Struct. Geol. 32, 1643–1655.
Gudmundsson, A., 2011a. Rock Fractures in Geological Processes. Cambridge University Press, Cambridge.
Gudmundsson, A., 2011b. Deflection of dykes into sills at discontinuities and magma-chamber formation. Tectonophysics 500, 50–64.
Gudmundsson, A., 2020. Volcanotectonics: Understanding the Structure, Deformation and Dynamics of Volcanoes. Cambridge University Press, Cambridge.
Gudmundsson, A., 2022. The propagation paths of fluid-driven fractures in layered and faulted rocks. Geol. Mag. 159, 1978–2001.
Gudmundsson, A., 2024a. How multiple dikes facilitate volcanic eruptions, with application to recent events on the Reykjanes Peninsula, Iceland. EGU24–12898, 2024. https://doi.org/10.5194/egusphere-egu24-12898.
Gudmundsson, A., 2024b. The effects of stress gradients on faulting and dike emplacement, with applications to Santorini and Iceland. EarthArXiv. https://doi.org/10.31223/X5KH8W.
Gudmundsson, A., Brenner, S.L., 2003. Loading of a seismic zone to failure deforms nearby volcanoes: a new earthquake precursor. Terra Nova 15, 187–193.
Gudmundsson, A., Brenner, S.L., 2004. How mechanical layering affects local stresses, unrests, and eruptions of volcanoes. Geophys. Res. Lett. 31. https://doi.org/10.1029/2004GL020083.
Gudmundsson, A., Brenner, S.L., 2005. On the conditions of sheet injections and eruptions in stratovolcanoes. Bull. Volcanol. 67, 768–782.
Gudmundsson, A., Homberg, C., 1999. Evolution of stress fields and faulting in seismic zones. Pure Appl. Geophys. 154, 257–280.
Gudmundsson, A., Philipp, S.L., 2006. How local stress fields prevent volcanic eruptions. J. Volcanol. Geotherm. Res. 158, 257–268.
Gudmundsson, A., Lecoeur, N., Mohajeri, N., Thordarson, T., 2014. Dike emplacement at Bardarbunga, Iceland, induces unusual stress changes, caldera deformation, and earthquakes. Bull. Volcanol. 76. https://doi.org/10.1007/s00445-014-0869-8.
Gudmundsson, A., Drymoni, K., Browning, J., Acocella, V., Amelung, F., Bonali, F.L., Abdelsalam, E., Galindo, I., Geshi, N., Geyer, A., Heap, M.J., Karaoğlu, O., Kusumoto, S., Marti, J., Pinel, V., Tibaldi, A., Thorvaldur Thordarson, T., Walter, T. R., 2022. Volcanotectonics: the tectonics and physics of volcanoes and their eruption mechanics. Bull. Volcanol. 84, 72. https://doi.org/10.1007/s00445-022-01582-4.
Hobe, A., Bazargan, M., Tryggvason, A., Alofe, E., Gudmundsson, A., 2025. Tomographic and volcanotectonic control on the 2021–2023 Fagradalsfjall eruptions, Iceland. Scientific Reports (in press).
Howard, G.C., Fast, C.R., 1970. Hydraulic Fracturing. Society of Petroleum Engineers of AIME, New York.
Iceland Meteorological Office, 2025. Ground Uplift and Magma Accumulation Continue Beneath Svartsengi. https://en.vedur.is/about-imo/news/magma-accumulation-beneath-svartsengi-continues.
Inskip, N.D.F., Browning, J., Meredith, P.G., Gudmundsson, A., 2020. Conditions for fracture arrest in layered rock sequences. Results Geophys. Sci. 1-4. https://doi.org/10.1016/j.ringps.2020.100001.
Jakobsson, S., 1979. Petrology of recent basalts of the eastern volcanic zone, Iceland. Acta Nat. Isl. 26, 1–103.
Jenness, M.H., Clifton, A.E., 2009. Controls on the geometry of a Holocene crater row: a field study from Southwest Iceland. Bull. Volcanol. 71, 715–728.
Jonsson, J., 1983. Eruptions during historic times on the Reykjanes Peninsula. Natturufraedingurinn 52, 127–139 (in Icelandic).
Moran, S.C., Newhall, C., Roman, D.C., 2011. Failed magmatic eruptions: late-stage cessation of magma ascent. Bull. Volcanol. 73, 115–122.
Neal, C.A., Brantley, S.R., Antolik, J.L., et al., 2019. The 2018 rift eruption and summit collapse of Kilauea Volcano. Science 363, 367–374.
Passarelli, L., Rivalta, E., Cesca, S., Aoki, Y., 2015. Stress changes, focal mechanisms, and earthquake scaling laws for the 2000 dike at Miyakejima (Japan). J. Geophys. Res. 120, 4130–4145.
Patrick, M.R., Dietterich, H.R., Lyons, J.J., et al., 2019. Cyclic lava effusion during the 2018 eruption of Kīlauea Volcano. Science 366, 1–10. https://doi.org/10.1126/science.aay9070.
Peltier, A., Ferrazzini, V., Staudacher, T., Bachelery, P., 2005. Imaging the dynamics of dyke propagation prior to the 2000-2003 flank eruptions at Piton de la Fournaise, Reunion Islands. Geophys. Res. Lett. 32. https://doi.org/10.1029/2005GL023720.
Pook, L.P., 2012. Crack Paths. WIT Press, London.
Reddy, J.N., 2002. Energy Principles and Variational Methods in Applied Mechanics, 2nd ed. Wiley, Hoboken, New Jersey.
Richards, T.H., 1977. Energy Methods in Stress Analysis. Ellis Horwood, Chichester.
Rivalta, E., Taisne, B., Bunger, A.P., Katz, R.F., 2015. A review of mechanical models of dike propagation: schools of thought, results and future directions. Tectonophysics 638, 1–42.
Roman, D.C., 2023. Global analysis of the relative timing of volcanic unrest and eruption Abstract. XXVIII Gen. Assembly Int. Union Geodesy Geophys. (IUGG). https://doi.org/10.57757/IUGG23-3088.
Rutherford, M.J., Gardner, J.E., 2000. Rates of magma ascent. In: Sigurdsson, H., et al. (Eds.), Encyclopedia of Volcanoes. Academic Press, pp. 207–217.
Saemundsson, K., 1991. The geology of the Krafla Volcanic System. In: Gardarson, A., Einarsson, A. (Eds.), Myvatn's Nature. Hid islenska Natturufraedifelag, Reykjavik (in Icelandic), pp. 24–95.
Sanford, R.J., 2003. Principles of Fracture Mechanics. Prentice-Hall, Upper Saddle River, New Jersey.
Segall, P., 2010. Earthquake and Volcano Deformation. Princeton University Press, Princeton.
Shapiro, S.A., 2018. Fluid-Induced Seismicity. Cambridge University Press, Cambridge.
Sigurdssson, O., 1977. Volcano-tectonic activity in the Thingeyjarthing county (II) 1976-1978. Tyli 7, 41–56 (in Icelandic with English summary).
Tauchert, T.R., 1981. Energy Principles in Structural Mechanics. Krieger, Malabar, Florida.
Thiele, S.T., Cruden, A.R., Zhang, X., Micklethwaite, S., Matchan, E.L., 2021. Reactivation of magma pathways: insights from field observations, geochronology, geomechanical tests, and numerical models. J. Geophys. Res. 126, e2020JB021477. https://doi.org/10.1029/2020JB021477.
Thordarson, T., Hoskuldsson, A., 2008. Postglacial volcanism in Iceland. Jokull (The Icelandic Journal of Earth Sciences) 58, 197–228.
Thordarson, T., Larsen, G., 2007. Volcanism in Iceland in historical time: volcano types, eruption styles and eruptive history. J. Geodyn. 43, 118–152.
Tibaldi, A., 2015. Structure of volcano plumbing systems: a review of multi-parametric effects. J. Volcanol. Geotherm. Res. 298, 85–135.
Townsend, M.R., Pollard, D.D., Smith, R.P., 2017. Mechanical models for dikes: a third school of thought. Tectonophysics 703=704, 98–118.
Troll, V.R., Deegan, F.M., Thordarson, T., et al., 2024. The Fagradalsfjall and Sundhnúkur fires of 2021–2024: a single magma reservoir under the Reykjanes Peninsula, Iceland? Terra Nova 00, 1–10. https://doi.org/10.1111/ter.12733.
Tryggvason, E., 1977. The volcanotectonic event in the Myvatn county in September 1977. Earthquake Lett. 25, 2–5 (in Icelandic).
Tryggvason, E., 1983. The widening of the Krafla fissure swarm during the 1975-1981 volcanotectonic episode. Nordic Volcanol. Instit. Prof. Pap. 8304, 48.
Tryggvason, E., 1984. Widening of the Krafla fissure swarm during the 1975-1981 volcanotectonic episode. Bull. Volcanol. 47, 47–69.
Valko, P., Economides, M.J., 1995. Hydraulic Fracture Mechanics. Wiley, New York.
Wu, Y.S. (Ed.), 2017. Hydraulic Fracture Modeling. Gulf Publishing, Houston.
Yew, C.H., Weng, X., 2014. Mechanics of Hydraulic Fracturing, 2nd ed. Gulf Publishing, Houston.